PHASE DIAGRAM OF KHF_2 AND NON-EQUILIBRIUM EFFECTS

FINAL REPORT

TASK 6 AND TASK 7

BY

MELVIN C. HOBSON

AND

JORDAN D. KELLNER

PREPARED UNDER CONTRACT NO. NAS 2-9273

BY

HAMILTON STANDARD
DIVISION OF UNITED AIRCRAFT CORPORATION
WINDSOR LOCKS, CONNECTICUT

FOR

NATIONAL AERONAUTICS AND SPACE ADMINISTRATION
AMES RESEARCH CENTER
MOFFETT FIELD, CALIFORNIA 94035

OCTOBER, 1978

CR 152192

HAMILTON STANDARD Division of UNITED TECHNOLOGIES

SVHSER 7206

R78-313686-8

PHASE DIAGRAM OF KHF_2 AND NON-EQUILIBRIUM EFFECTS

FINAL REPORT

TASK 6 AND TASK 7

BY

MELVIN C. HOBSON

AND

JORDAN D. KELLNER

PREPARED UNDER CONTRACT NO. NAS 2-9273

BY

HAMILTON STANDARD
DIVISION OF UNITED AIRCRAFT CORPORATION
WINDSOR LOCKS, CONNECTICUT

FOR

NATIONAL AERONAUTICS AND SPACE ADMINISTRATION
AMES RESEARCH CENTER
MOFFETT FIELD, CALIFORNIA 94035

OCTOBER, 1978

CR 152192

HAMILTON STANDARD Division of UNITED TECHNOLOGIES

SVHSER 7206

R78-313686-8

ABSTRACT

Phase Diagram of KHF_2 and Non-Equilibrium Effects

Final Report
Task 6 and 7
by
Melvin G. Hobson, Jr.
and Jordan D. Kellner

Contract No. NAS2-9273

This report describes the method, results and theoretical interpretation of a determination of the phase diagram of the potassium bifluoride-water system. The effect of non-equilibrium conditions such as a rapid cooling rate on the phase behavior was also determined and evaluated as it effected the practical use of the system as a high capacity heat absorber.

FOREWORD

This document has been prepared by the United Technologies Research Center for Hamilton Standard Division of United Technologies Corporation and for the National Aeronautics and Space Administration's AMES Research Center in accordance with the requirements of Contract NAS2-9273, Fusible heat sink for EVA, Tasks 6 and 7.

United Technologies Research Center personnel responsible for the conduct of this program were Hal Couch, Section Chief, Jordan D. Kellner, Supervisor and Melvin C. Hobson, Senior Research Scientist.

INTRODUCTION

During effort funded by NASA/ARC under Contract NAS2-8665 the heat absorption capacity of the potassium bifluoride-water (KHF_2-H_2O) system was found to be large, 530 J/g (228 Btu/lb) for the 20% KHF_2 solution (Reference 1); however, this capacity seemed to be dependent on the particular rate and method of freezing. The KHF_2 solubility is very dependent on temperature, decreasing from 39.2 g/100g (.39 lb/lb H_2O) H_2O at 20°C (68°F) to about 20g/100g (.2 lb/lb H_2O) H_2O at 5°C (41°F). Therefore, KHF_2 was expected to be precipitated first during the regeneration step. The existence of hydrates that might form on freezing the solution or the existence of metastable states, supersaturation effects, etc., would have a strong effect on the heat absorption of the system during melting. A determination of the equilibrium phase diagram for the system would uncover any unexpected behavior and might help to explain the heat absorption anomolies. A second investigation to determine the effect of rapid freezing on the phase behavior in order to more closely approximate actual regeneration procedures might also help to explain the heat absorption anomolies. Therefore, a program to establish the equilibrium and non-equilibrium phase diagram was initiated.

This report covers the effort conducted at United Technologies Research Center under NASA/ARC Contract NAS2-9273 to determine the phase diagram and non-equilibrium effects of the potassium bifluoride-water system.

SUMMARY

The equilibrium diagram for the KHF_2-H_2O system was constructed from cooling and heating curves for the compositions between 5 wt% and 40 wt% KHF_2 and the results are shown in Figure 12. The phase diagram shown in the figure is typical of that of a two component system with miscible liquid phases and whose solid phases consist of pure components. A eutectic point was found at approximately 15% KHF_2 which remains completely liquid down to a temperature of -9.0°C (15.8°F). No hydrate formation was observed and no anomolous behavior such as the occurrence of solid transitions or metastable states was observed. The effect of rapid freezing on the phase diagram was determined to be confined chiefly to the hypereutectic compositions. At these concentrations, the first transition observed on the equilibrium diagram did not appear, and the cooling curves exhibited only one halt. Also, at rapid freezing rates, the supercooling of the solutions was smaller than those observed at the slow cooling rates.

The existence of a eutectic composition and the slow rate of dissolution of the salt are used to interpret heat absorption behavior in practical applications of the KHF_2-H_2O system.

CONCLUSIONS

1. The equilibrium phase diagram for the KHF_2-H_2O system exhibits simple eutectic type behavior with no hydrate formation.

2. A eutectic mixture of 15% KHF remains completely liquid down to a temperature of -9°C (15.8°F).

3. Rapid freezing of the 20% KHF_2 solution causes eutectic type solidification. This same type of solidification is exhibited by the 15% solution at all freezing rates. This solidification results in the most intimate mixing of salt and water-ice.

4. Supercooling for hypoeutectic solutions decreases as the freezing rate increases but supersaturation for hypereutectic solutions increases as the freezing rate increases.

5. The probable cause of anomolous heat absorption behavior for the 20% KHF_2 solution observed previously is slow dissolution of the salt due to the relatively high temperature for the liquidus curve.

6. High freezing rates cause a more intimate, finely divided mixture of salt and water-ice to precipitate from hypereutectic solutions than slow freezing rates. Therefore, more efficient heat absorption upon melting is expected from fast frozen mixtures due to the faster dissolution of salt from finely divided crystals.

RECOMMENDATIONS

1. The heat absorption measurement for the eutectic composition should be performed in a calorimeter apparatus and in a larger scale apparatus to determine the effect on the kinetics of dissolution of the much lower liquidus temperature for this solution.

2. The possibility that other salt systems exist with properties similar or exceeding those of KHF_2 but with higher dissolution rates should be investigated.

TABLE OF CONTENTS

LIST OF FIGURES

LIST OF TABLES

PROGRAM OUTLINE

The phase behavior study of the KHF_2-H_2O system covered by this report includes:

1) A construction of the equilibrium diagram from cooling curves of solutions between 5 and 40 weight % KHF_2.

2) The effect of cooling rate on the phase diagram determined by sampling phases that occur in the solutions at higher cooling rates and comparing the results with the equilibrium phases at the temperatures determined previously.

3) An interpretation of the results as they apply to the anomolous heat absorption behavior of the KHF_2-H_2O system.

DESCRIPTION OF EXPERIMENTAL APPARATUS

A cold bath filled with methanol was used to control the temperature of the KHF_2 solutions. The capacity was 7.6 liters (two gallons) with temperature regulation by a thermistor probe that can hold the bath temperature to within ±.02°C (±.036°F) through a range of -25°C (-13°F) to 150°C (302°F). The KHF_2 solutions in a stainless steel beaker, were suspended in the methanol bath.

The temperature within the sample in the stainless steel beaker was monitored by a ten thermocouple thermopile which delivered a potential of 0.37 mv/degree to a recorder. The thermopile is distributed in the beaker in a circular pattern shown in Figure 1 so that the thermocouple junctions sample different parts of the KHF_2 solution. However, temperature sampling problems do persist because the thermocouples are all the same distance from the beaker/cold bath interface, and therefore solid that starts forming at that interface upon cooling of the solution is not immediately sampled. This delay can be minimized by running heating curves as well as cooling curves especially to determine eutectic transition points. This procedure is known as the freeze-thaw method.

The beaker top is covered with clear lucite in which the thermocouple lead-in wires are mounted in order to visually observe the onset of phase transitions.

Chemical analysis by quantitative determination of potassium ion was used to determine the composition of liquid and solid phases.

The solid phase samples were purified by several freeze-thaw cycles at the freezing point of the solution. X-ray defraction patterns were obtained on the solid phases using $Cu_{K\alpha}$ radiation to search for possible compound formation.

The solutions were prepared from stock KHF_2 obtained from American Hoechst Corp., New Jersey, after the material was dried sufficiently to produce a constant weight at 120°C (248°F) (about 24 hours). The chemical analysis by potassium determination on stock solutions is shown in Table I.

A sampling error for the 40% solution resulted in a low value since the solubility limit is only about 30% for the KHF_2-H_2O system. Therefore, in order to obtain a true analysis, a uniform suspension of KHF_2 solid and KHF_2 solution would have to be sampled. Some solid was left behind and a lower value for KHF_2 concentration resulted.

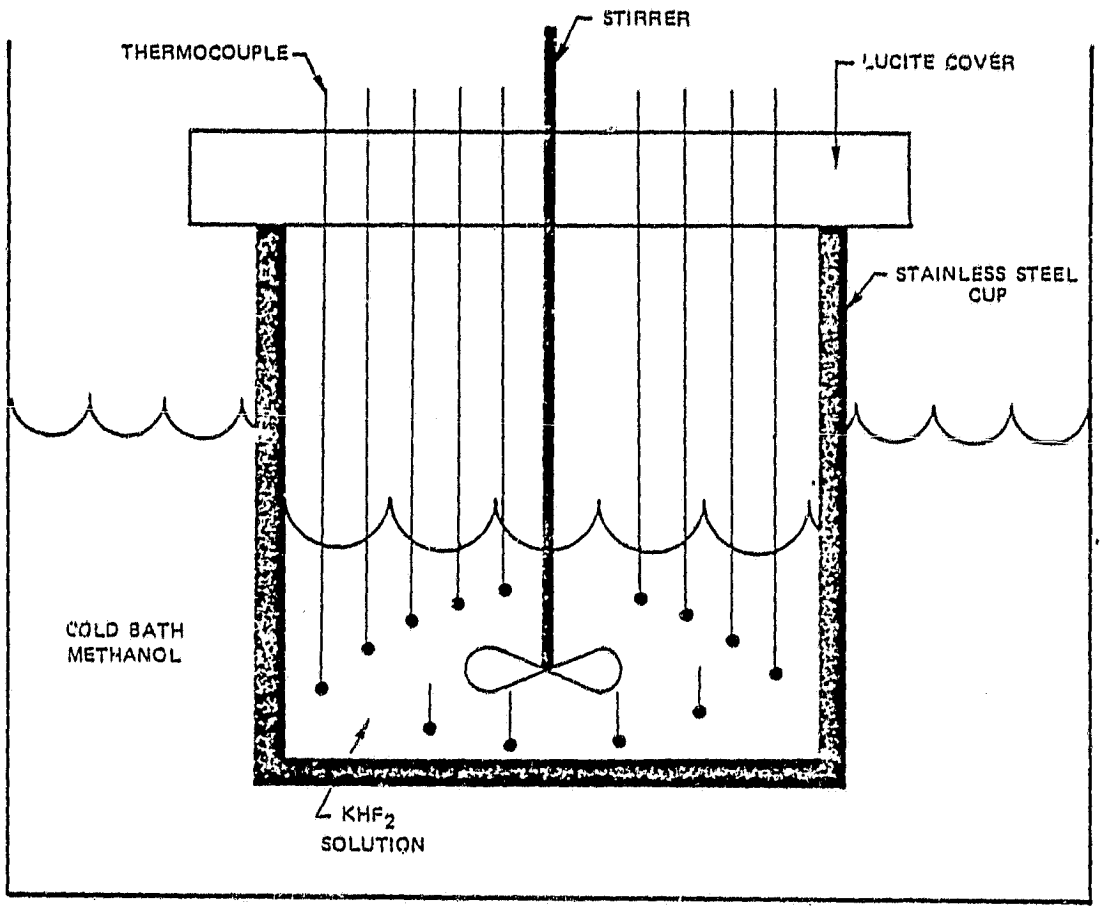

ORIGINAL PAGE IS
OF POOR QUALITY

FIG. 1

78-07-191-1

TABLE I

CHEMICAL ANALYSIS OF STOCK KHF_2 SOLUTION COMPOSITION wt%

NOMINAL	ANALYSIS
5	4.98
10	9.56
13	12.3
15	14.4
18	18.4
20	19.7
25	23.8
40	31.4

RESULTS

The results obtained are presented in the form of cooling curves, analyses, visual observations and theoretical analyses. These results are discussed in terms of equilibrium phase diagram determination, and non-equilibrium effects.

Equilibrium Diagram Determination

Cooling curves for 5, 10, 20, 25, 30 and 40 wt percent solutions are presented in Figures 2, 3, 4, 5, 6 and 7, respectively. When it became apparent that the composition region between 10 and 20% was of greatest interest because of the discovery of a eutectic point, the solutions of 13, 15 and 18 percent were measured and are shown in Figures 8, 9 and 10.

The 5% solution exhibited supercooling since the temperature was lowered 3.5°C (6.3°F) below the freezing point before any solid material appeared as shown in Figure 2. The dashed line in all cooling curves represents the path of temperature readings if no supercooling had taken place. The freezing point for the 5% solution was -2.6°C (27.3°F). The fact that the first solid to appear precipitated at a temperature below that of the freezing point of water indicates that the solid phase is solvent and the 5% KHF_2 solution causes a

TEMPERATURE VERSUS TIME FOR 5% KHF_2

SLOW COOLING

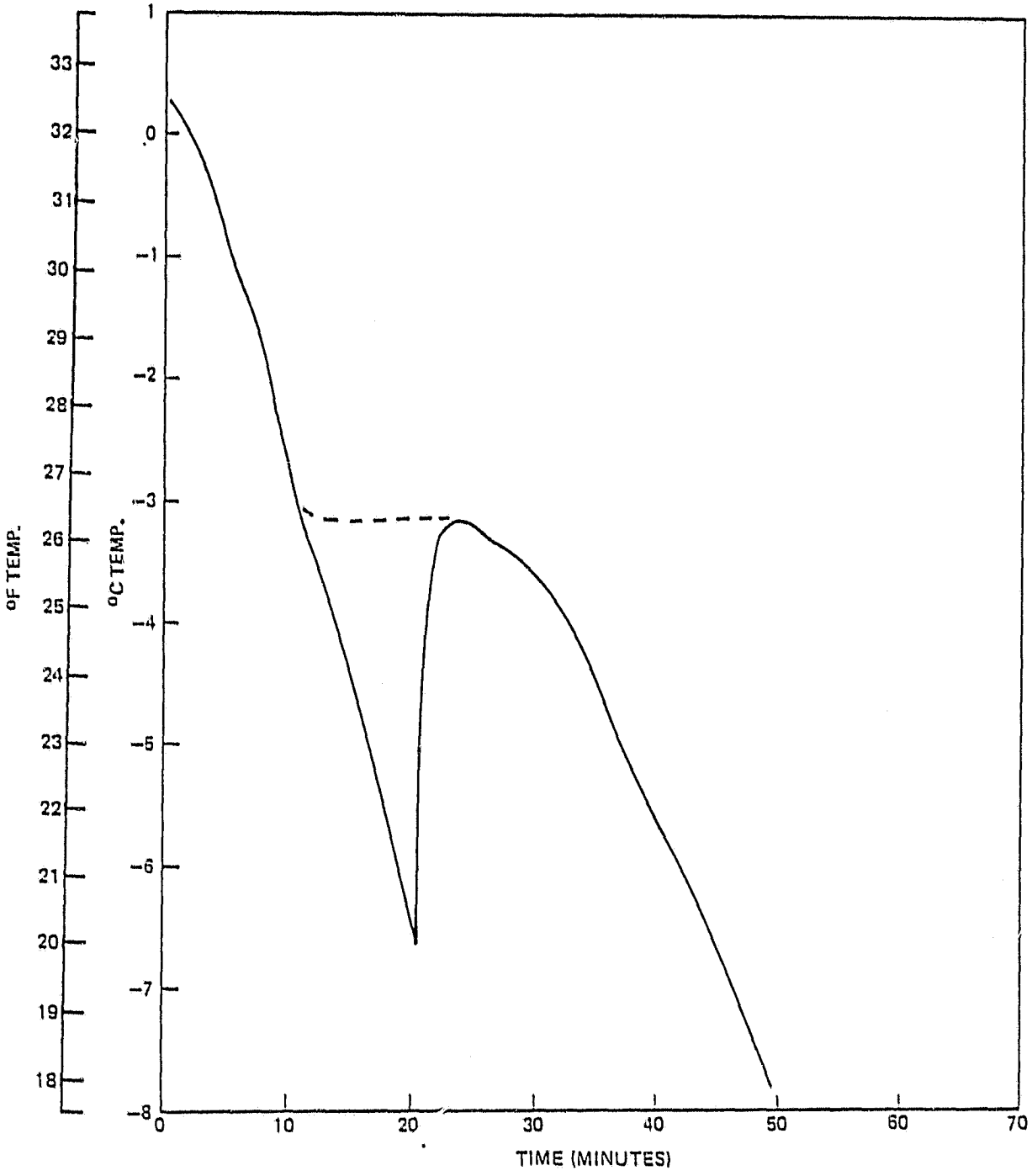

FIG. 2

78-02-98-1

SLOW COOLING

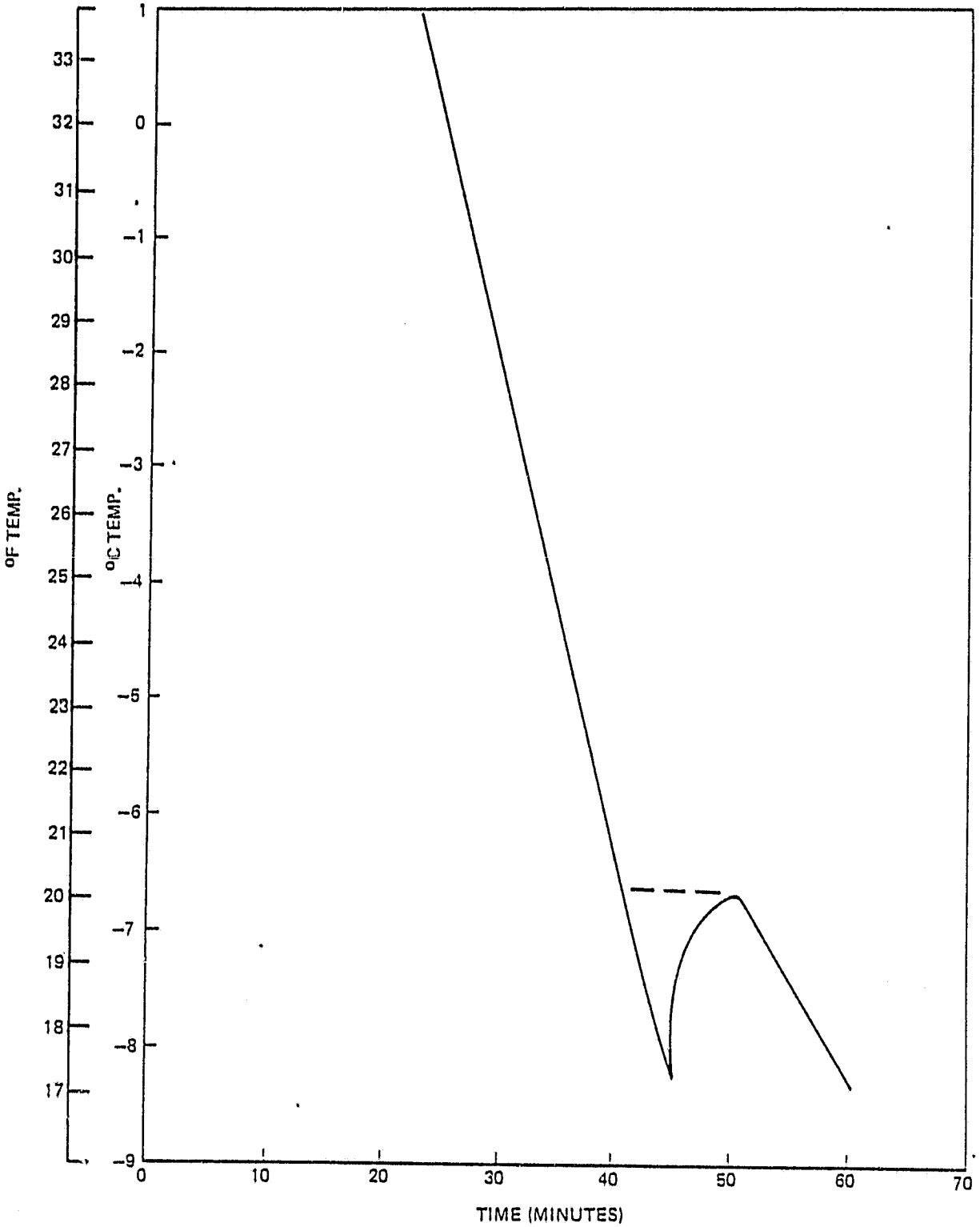

FIG. 3

78-02-98-2

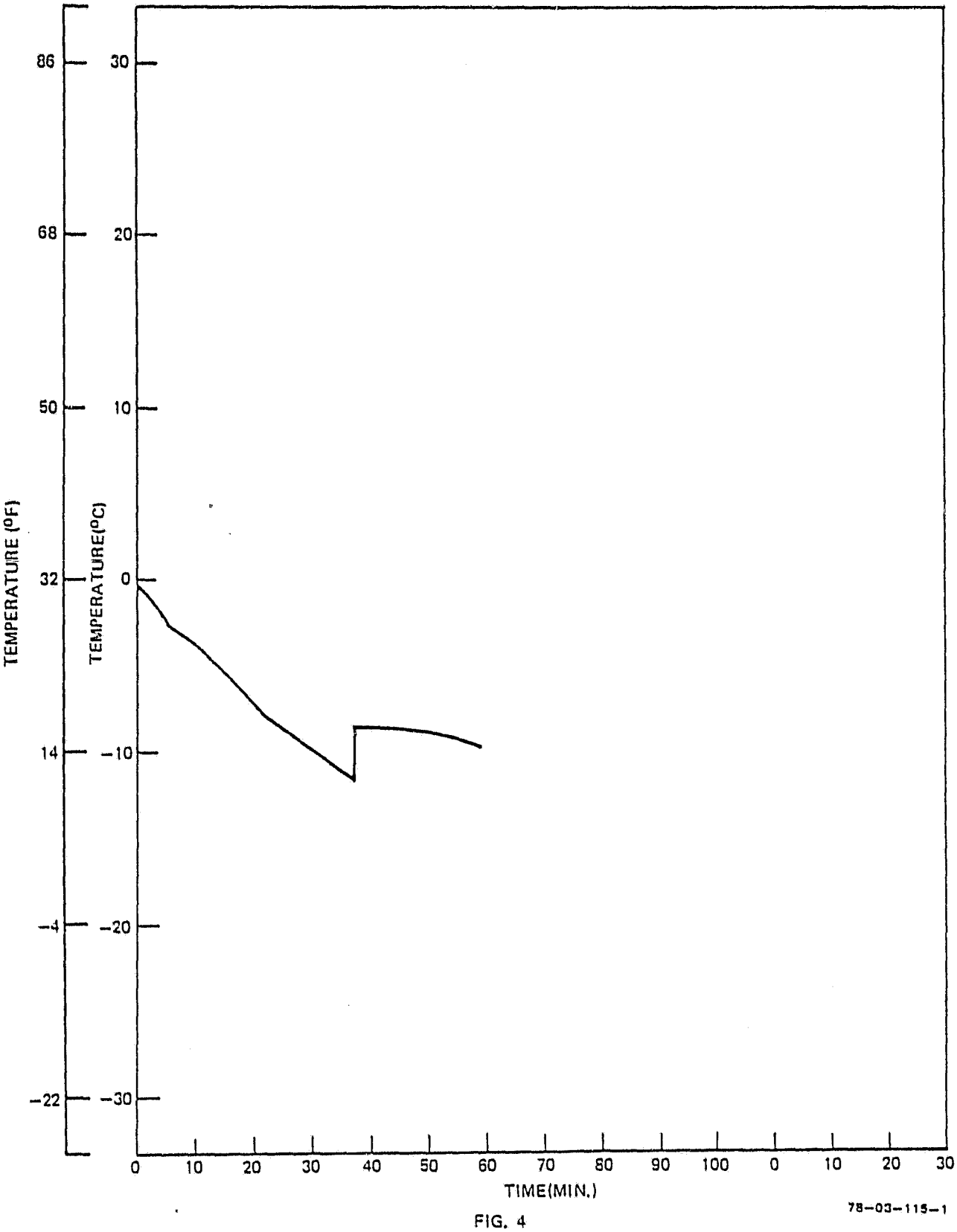
TEMPERATURE (°F)
TEMPERATURE(°C)
86
68
50
32
14
-4
-22
30
20
10
0
-10
-20
-30
0
10
20
30
40
50
60
70
80
90
100
0
10
20
30
TIME(MIN.)
78-03-115-1

FIG. 4

TEMPERATURE VERSUS TIME FOR 25% KHF_2

SLOW COOLING

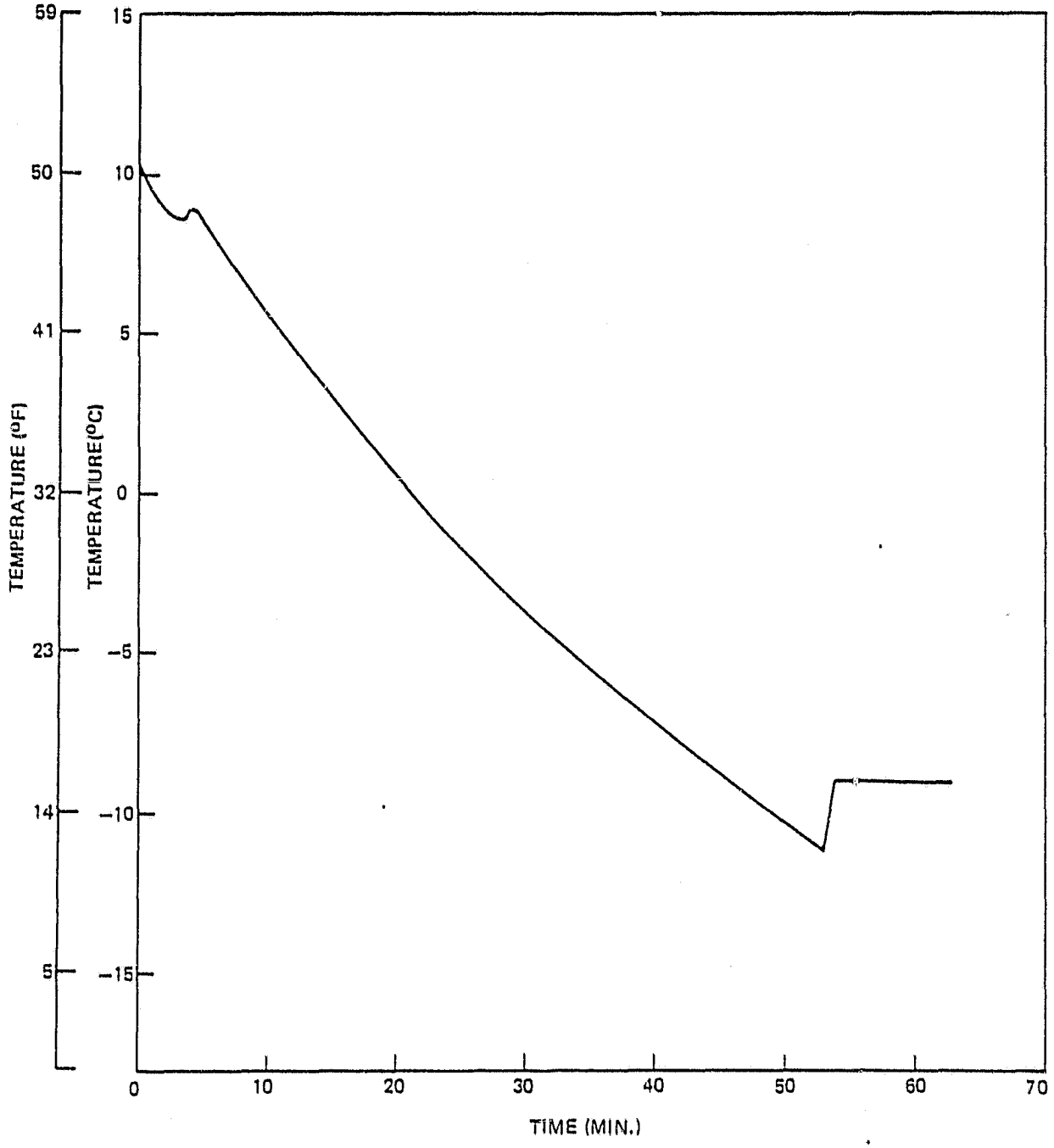

FIG. 5

78-04-61-2

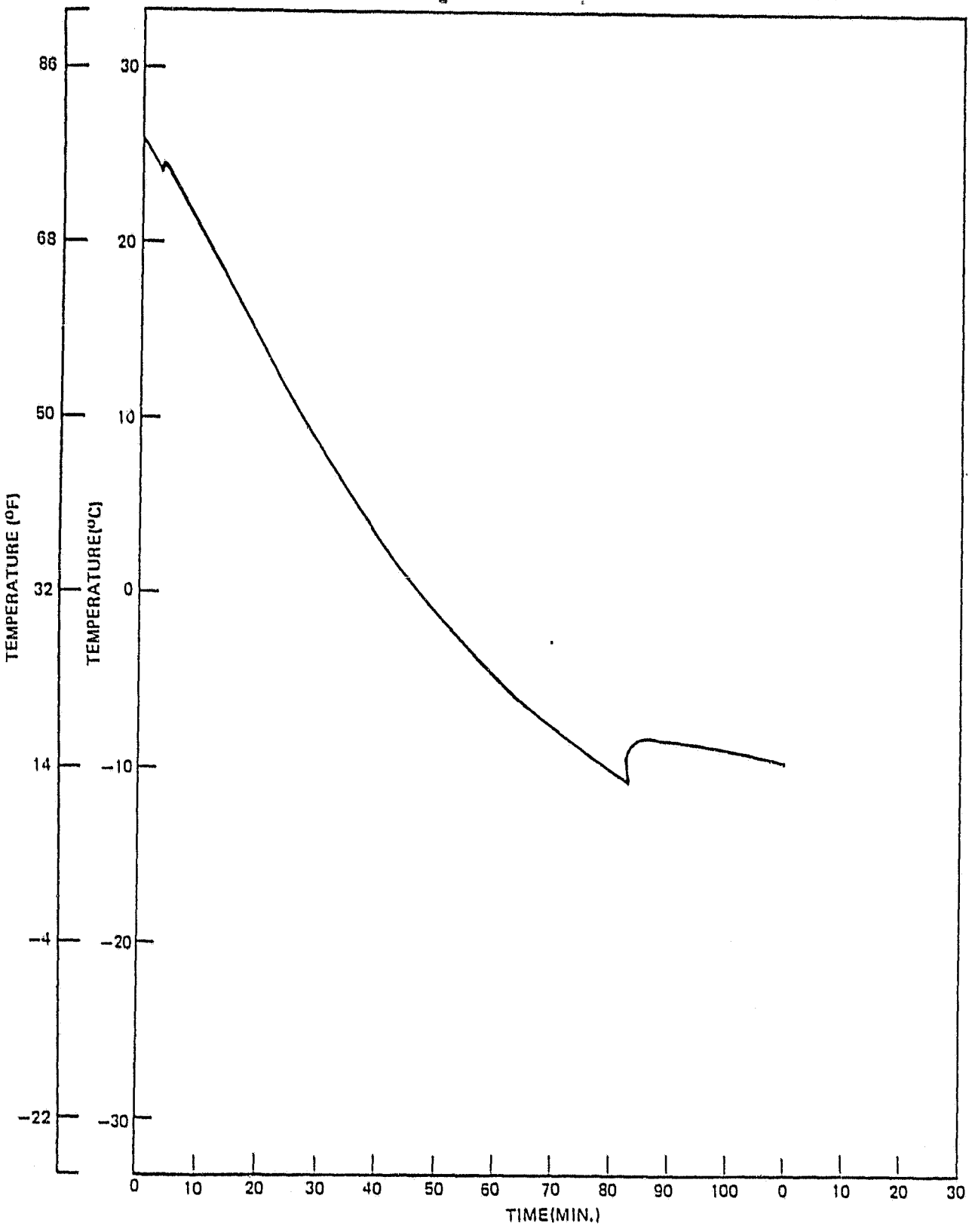

FIG. 6

78-03-115-2

TEMPERATURE VERSUS TIME FOR 40% KHF_2

SLOW COOLING

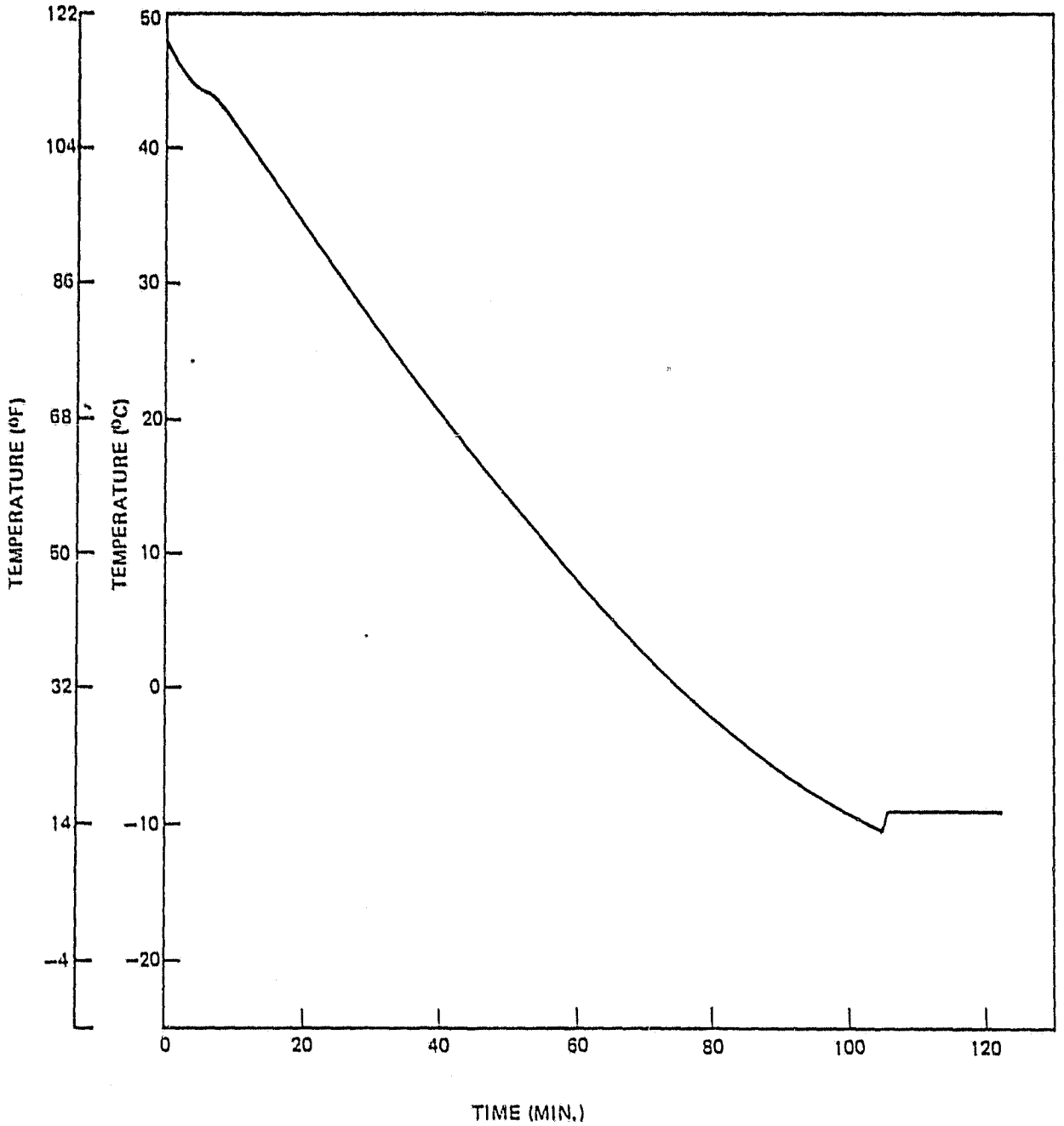

FIG. 7

78-04-61-2

TEMPERATURE VERSUS TIME FOR 13% KHF_2

SLOW COOLING

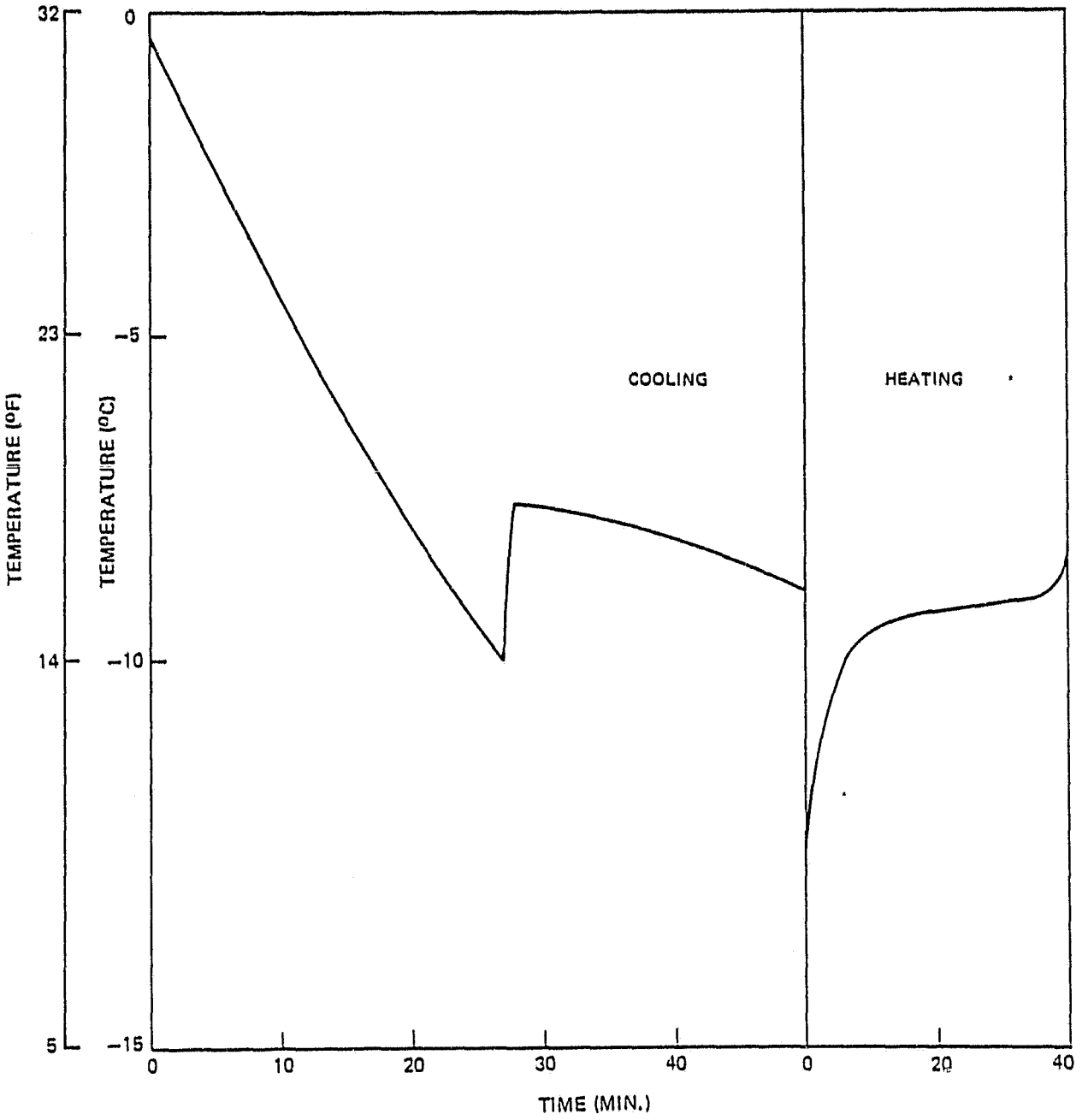

FIG. 8

78-04-61-7

TEMPERATURE VERSUS TIME FOR 15% KHF_2

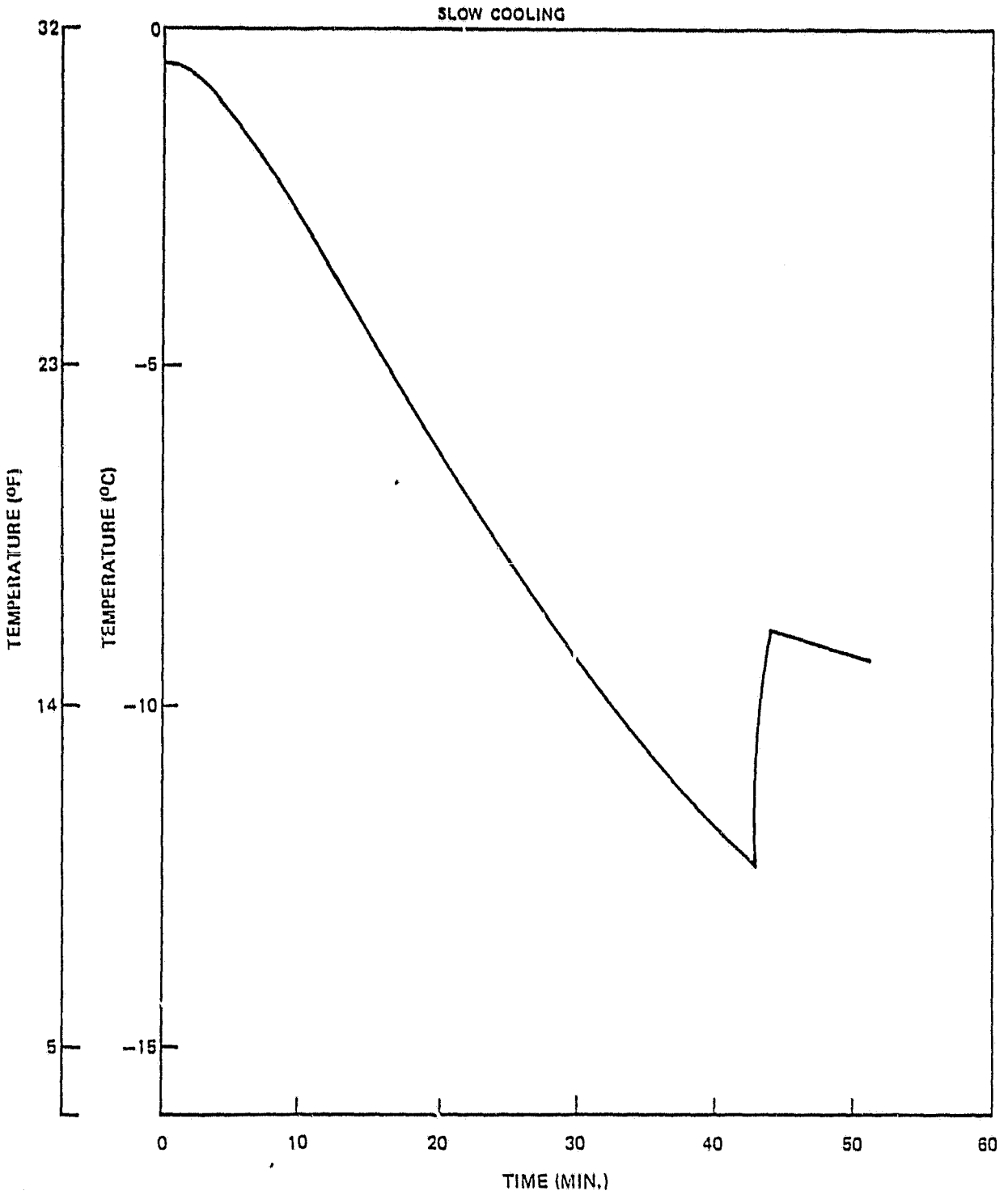

FIG. 9

78-04-61-6

TEMPERATURE VERSUS TIME FOR 18% KHF_2

SLOW COOLING

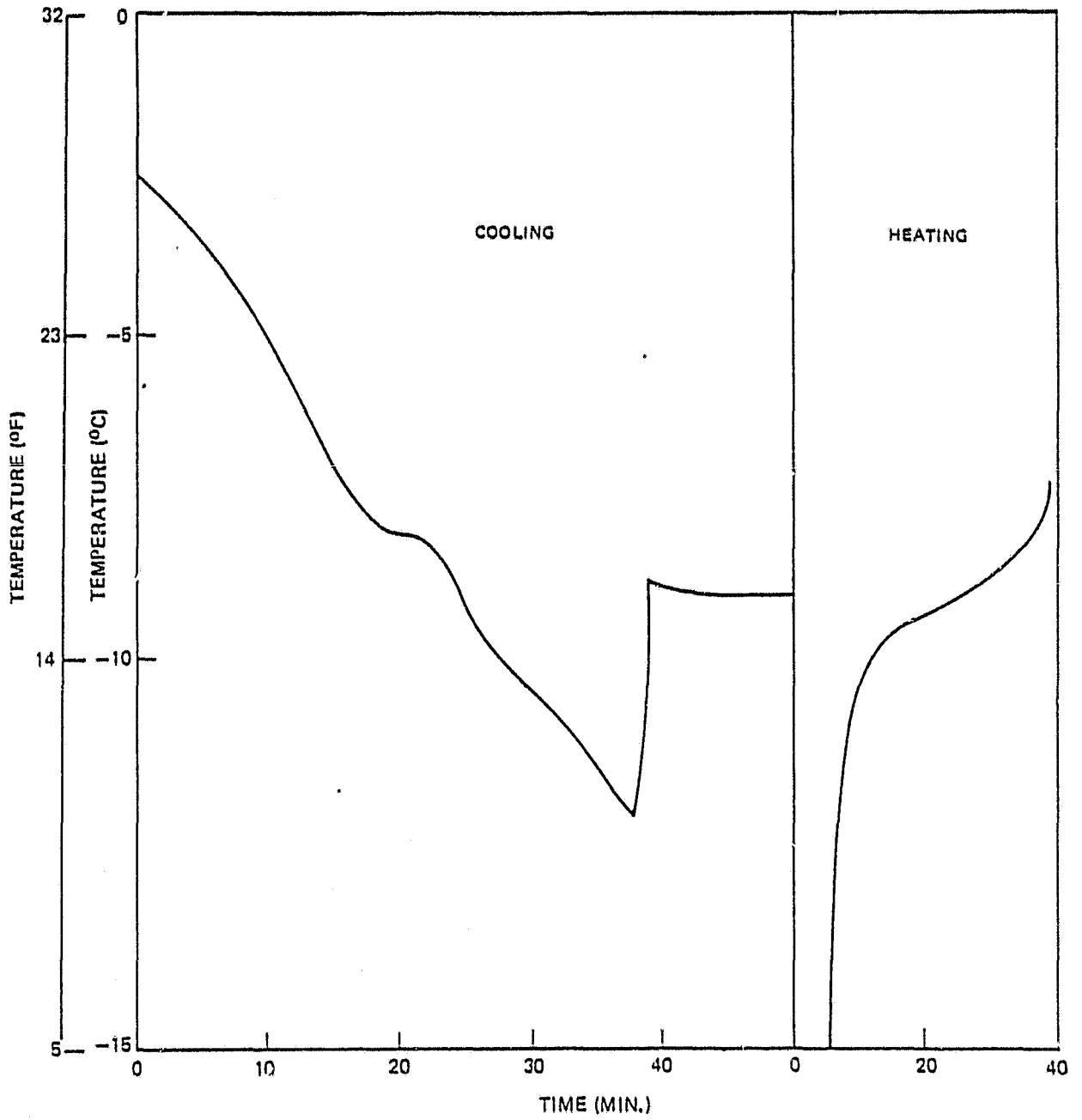

FIG. 10

78-04-61-1

freezing point depression of -2.6°C (4.7°F). To check this result and to determine the degree of dissociation of KHF_2, the theoretical freezing point depression was calculated assuming Raoult's law behavior for the solvent.

In a dilute solution the solvent obeys Raoult's law and behaves ideally as expressed by the equation,

$$\left(\frac{\partial \ln N_1}{\partial T}\right)_P = \frac{\Delta H_f}{RT^2} \qquad (1)$$

where N_1 = mole fraction of the solvent.
ΔH_f = molar heat of fusion of solid solvent.
R is the gas constant
T is absolute temperature

Equation (1) applies at the freezing point of a dilute solution in equilibrium with solid solvent. Integration between temperature limits of the freezing point of the pure solvent and the freezing point of the solution gives,

$$\ln N_1 = \frac{\Delta H_f}{R} \frac{T - T_o}{(T\ T_o)} \qquad (2)$$

where T_o = freezing point of pure solvent.
T = freezing point of solution.

For dilute solutions $\ln N_1$ approximates $N_1 - 1$ and $(T\ T_o)$ approximates T_o^2. Since $-N_2 = N_1 - 1$, the equation can be rewritten as

$$N_2 = \frac{\Delta H_f}{R\ T_o^2}\ \Delta T \qquad (3)$$

Therefore, the mole fraction or wt% of solute is found to be directly proportional to the depression in the freezing point of the solvent. The freezing point depression expected for KHF_2 solutions assuming that the KHF_2 dissociates to K^+ and HF_2^- ions only was calculated using Equation (3) with the results shown in Table 2. Since there are twice as many ions as molecules of KHF_2, the total mole fraction of ions is approximately double the KHF_2 concentration. The calculated freezing points are compared to the actual freezing points determined from the cooling curves of Figures 2-10 in the last two columns of Table 2. The deviation from ideal, i.e., complete dissociation, is negligible at 5% but increases at the higher concentrations up to the eutectic point. Beyond the eutectic composition, (15%) the Raoult's relationship is no longer valid as indicated in the table and by Figure 11. Figure 11 compares the freezing point depression computed from Equation (3) to the measured depression obtained up to 20 wt% KHF_2. The value of the freezing point depression for the 20% KHF_2 solution is not similar to the theoretical depression because the solid appearing at this temperature is not solvent but solute. At 18% the deviation is the same as at 15% but it is of a different sign. These considerations and the results of the chemical analyses performed and described later, indicate that the phase diagram up to 15% KHF_2 is of a 100% ionized salt in water, with little or no solvent-solute interaction.

A second halt in the cooling curves in this composition range was not observed; however, it is often obscured because the system contains a large proportion of solid and stirring is difficult. Also, solid adheres to the thermocouples and so that a true equilibrium temperature is not recorded. For these reasons, the thaw-melt method of H. Reinboldt (Reference 2) was used which involves heating the mixtures. The temperature at which the first liquid appears when heating the frozen mixture is the eutectic point and the temperature where solid completely disappears is the freezing point or first halt in the cooling curve. The transition points for each concentration are shown in Table 3.

All compositions show a halt at the eutectic temperature which appears to be -8.7°C (16.3°F) $\pm$.5°C (.9°F). For those compositions above 15% KHF_2 the first transition represents the precipitation of salt since the chemical analyses show that the liquid composition is constant at about 15% at the eutectic temperature, as shown in Table 4. At concentrations greater than the eutectic composition, the liquid sampled at the first transition showed a lower concentration of KHF_2 indicating that the solid precipitate was salt, leaving behind less concentrated solutions.

HAMILTON STANDARD — Division of United Technologies

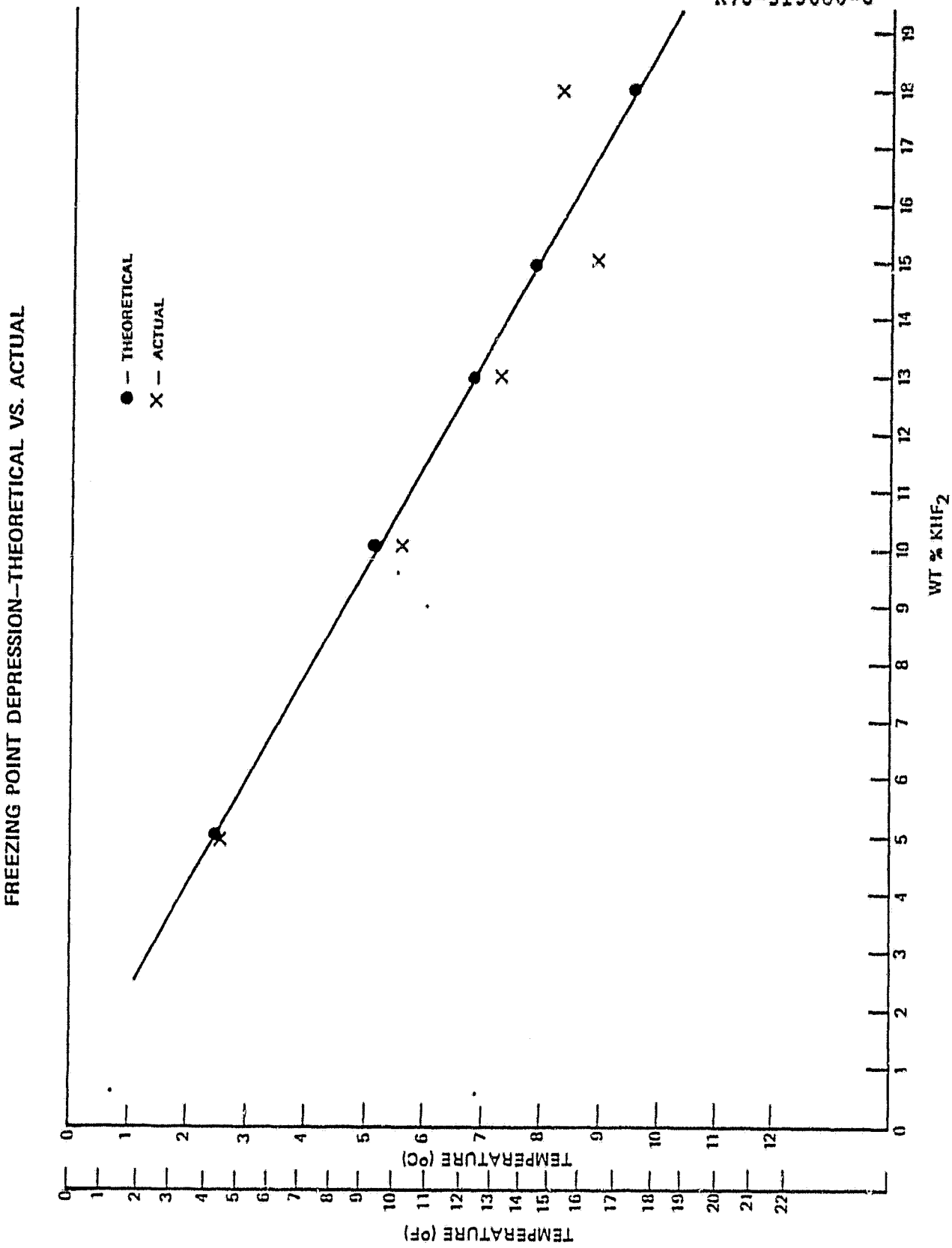

FIG. 11

TABLE 2

FREEZING POINT DEPRESSION FOR DILUTE KHF_2 SOLUTIONS

WT%	Concentration Mole Fraction	Mole Fraction of Ions	Freezing Point Depression °C	Freezing Point Depression (°F)	Calculated Freezing Point °C	Calculated Freezing Point (°F)	Measured Freezing Point °C	Measured Freezing Point (°F)
5	.012	.0237	2.5	(4.5)	-2.5	(27.5)	-2.6	(27.3)
10	.025	.0487	5.1	(9.2)	-5.1	(22.8)	-5.6	(21.9)
13	.033	.0644	6.8	(12.2)	-6.8	(19.8)	-7.3	(18.9)
15	.039	.0752	7.9	(14.2)	-7.9	(17.8)	-8.9	(16.0)
18	.048	.092	9.5	(17.1)	-9.5	(14.9)	-8.3	(17.1)
20	.055	.103	10.9	(19.6)	-10.9	(12.4)	-3.2	(26.2)

TABLE 3 - TRANSITION POINT TEMPERATURES

COMPOSITION, wt%	FIRST TRANSITION		EUTECTIC TRANSITION	
	°C	(°F)	°C	(°F)
5	-2.6)	(27.3)	-7.7	(18.1)
10	-5.6)	(21.9)	-9.1	(15.6)
13	-7.3)	(18.9)	-9.2	(15.4)
15	-8.9)	(16.0)	-8.9	(16.0)
18	-8.3)	(17.1)	-8.8	(16.2)
20	-3.2)	(26.2)	-8.0	(17.6)
25	9.0)	(48.2)	-8.8	(16.2)
30	23.4)	(74.1)	-8.6	(16.5)
40	44.3)	(111.7)	-8.9	(16.0)

TABLE 4

ANALYSIS OF LIQUID PHASES AT TRANSITION POINTS

COMPOSITION, wt%	Analysis, wt% LIQUID AT EUTECTIC TEMP	Analysis, wt% LIQUID AT FIRST TRANSITION
5		5.4
10		9.9
13		12.2
15	14.8	
18	15.4	
20	16.0	
25	15.8	
30		11.8
40	15.0	27.8

The X-ray diffraction pattern for the solid recovered at the first transition from 20 to 30% solutions was shown to be that of KHF_2 by matching with the ASTM standard X-ray pattern for this compound.

Based on the X-ray diffraction patterns, chemical analyses, Rauolt's law calculations and visual observations, the equilibrium phase diagram was constructed as shown in Figure 12.

Non-Equilibrium Effects On Phase Diagram

The cooling rate was increased from about 0.3°C/min (0.5°F/min) to 3-4°C/min (5.4-7.2°F/min) for the cooling curves shown in Figures 13-20 for the compositions 5, 10, 13, 15, 16, 18, 19 and 25 wt% KHF_2. The cooling rate of 0.3°C/min (0.5°F/min) is designated the slow or equilibrium rate since the cooling curves did not change with cooling rate in this range, and the 3-4°C/min (5.4-7.2°F/min) cooling rate is designated a moderate cooling rate. The cooling curves shown in Figures 21-30 for the compositions 5, 10, 15, 16, 18, 19, 20, 25, 30 and 40 wt% were obtained at cooling rates of 14°C/min (25.2°F/min) and are designated fast cooling rates. The most noticeable difference in the cooling curves for the non-equilibrium conditions is the larger degree of supercooling observed at the slower cooling rates. A summary of the degree of supercooling obtained under all three conditions is shown in Table 5.

TABLE 5

DEGREE OF SUPERCOOLING °C (°F)

	SLOW COOLING		MODERATE COOLING		FAST COOLING	
Composition, wt%	First Trans	Eutectic	First Trans	Eutectic	First Trans	Eutectic
5	2.7 (4.9)		0.6 (1.1)		0	
10	4.7 (8.5)		0.7 (1.3)		0	
13	4.0 (7.2)		0.9 (1.6)			
15		3.5 (6.3)		0.4 (0.7)		
16		3.3 (5.9)		0.4 (0.7)		
18	0	3.6 (6.5)		1.5 (2.7)		
19	0	2.2 (4.0)	0.5 (0.9)	0.9 (1.6)		
20	0	3.3 (5.9)			0.5 (0.9)	0.2 (0.4)
25	0	3.5 (6.3)	0.2 (0.4)	0.6 (1.1)	0	0.1 (0.2)
30					0.5 (0.9)	0
40					1.5 (2.7)	0

PHASE DIAGRAM OF THE KHF_2–H_2O SYSTEM

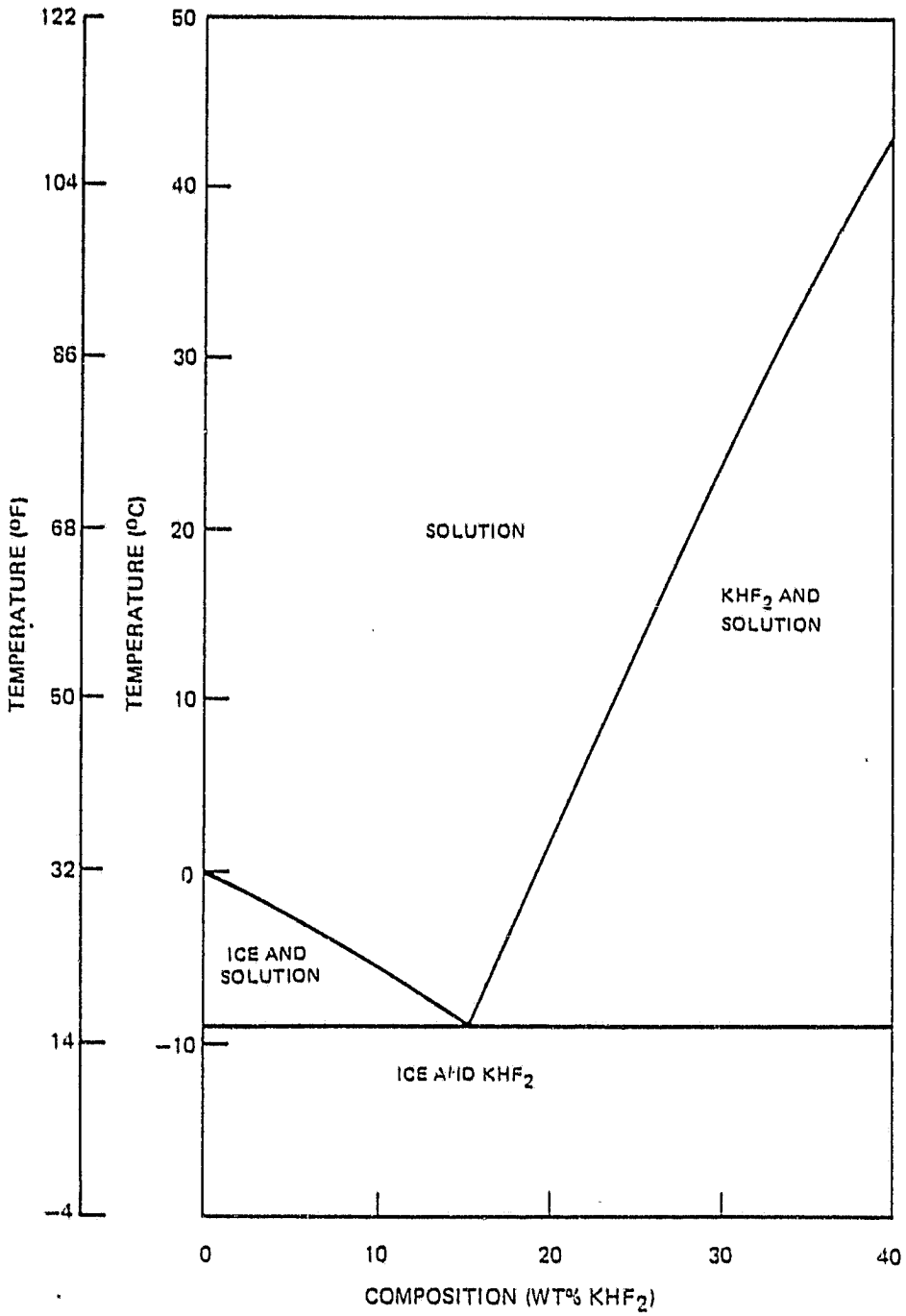

FIG. 12

78-04-61-5

TEMPERATURE VERSUS TIME FOR 5% KHF_2

MODERATE COOLING

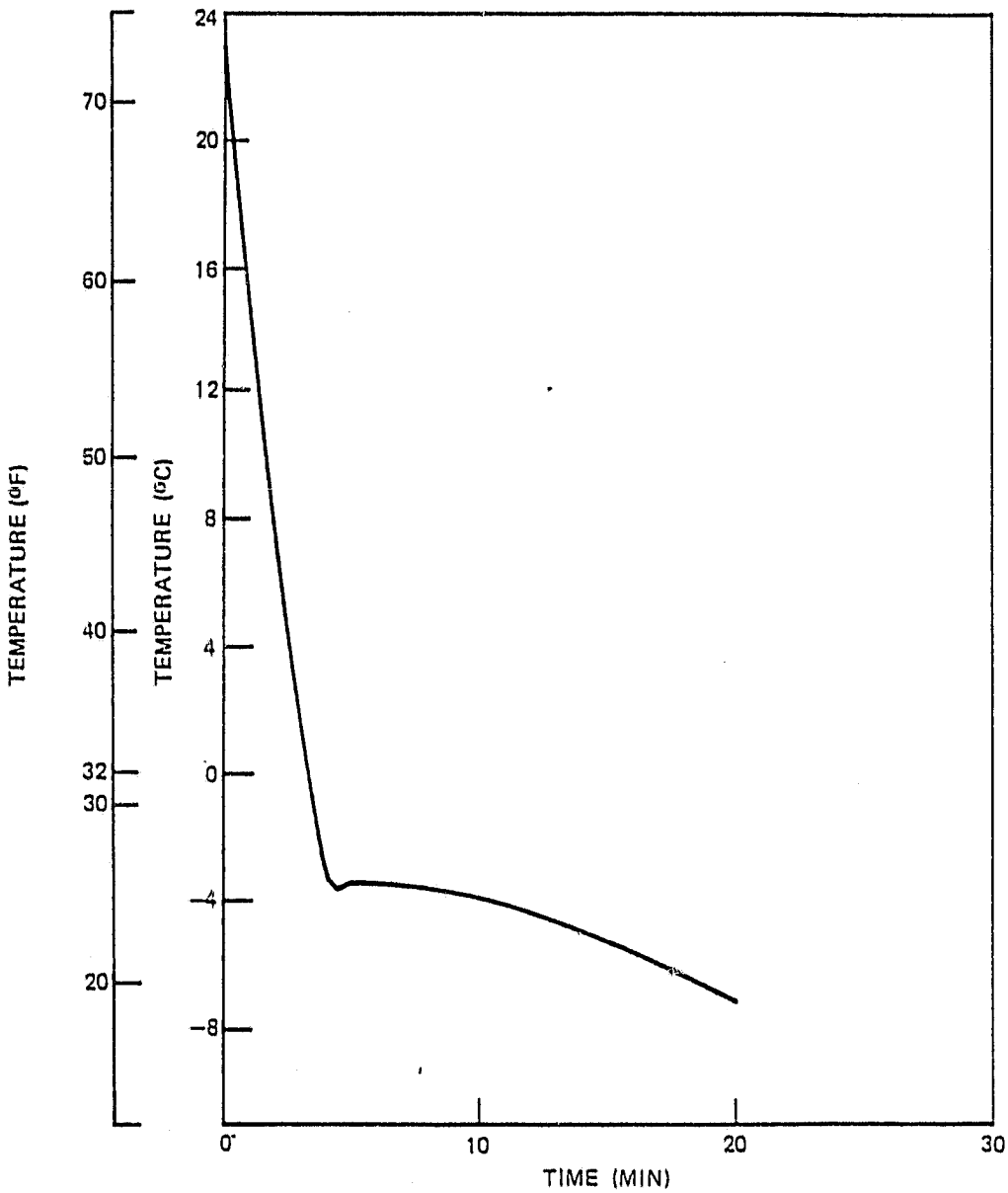

FIG. 13

78-05-55-1

TEMPERATURE VERSUS TIME FOR 10% KHF_2

MODERATE COOLING

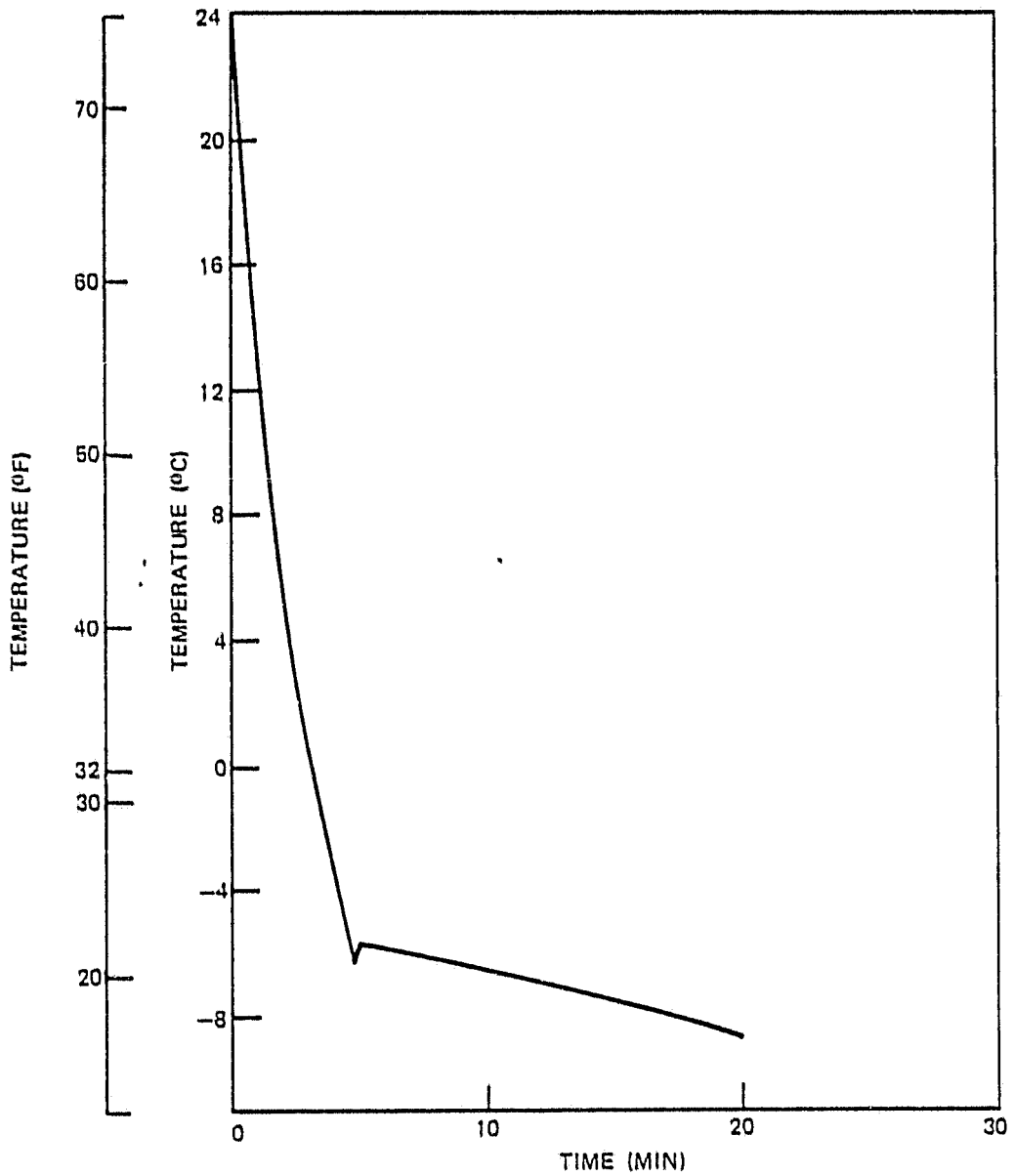

FIG. 14

78-05-55-2

TEMPERATURE VERSUS TIME FOR 13% KHF_2

MODERATE COOLING

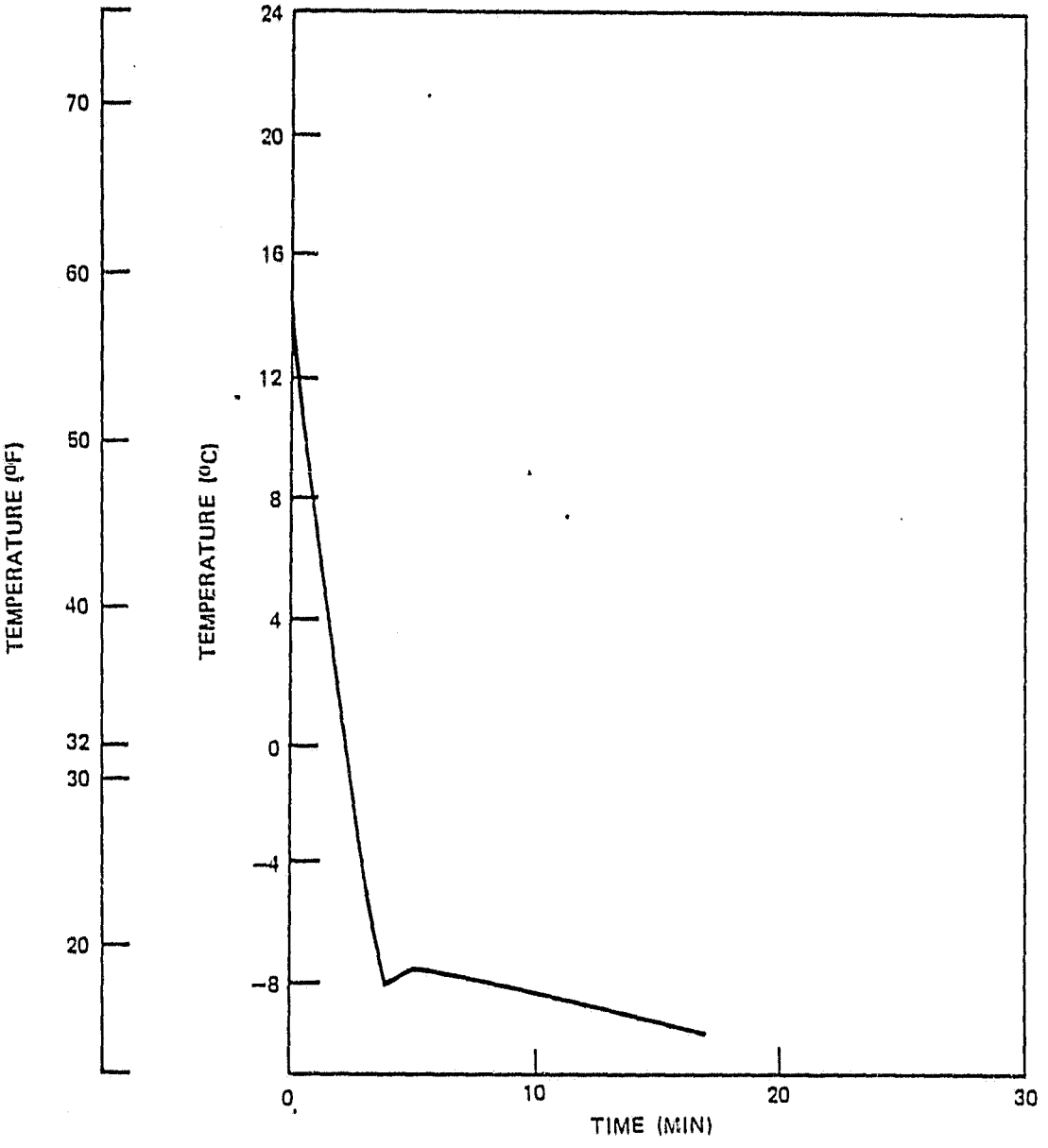

FIG. 15

78-05-55-3

TEMPERATURE VERSUS TIME FOR 15% KHF_2

MODERATE COOLING

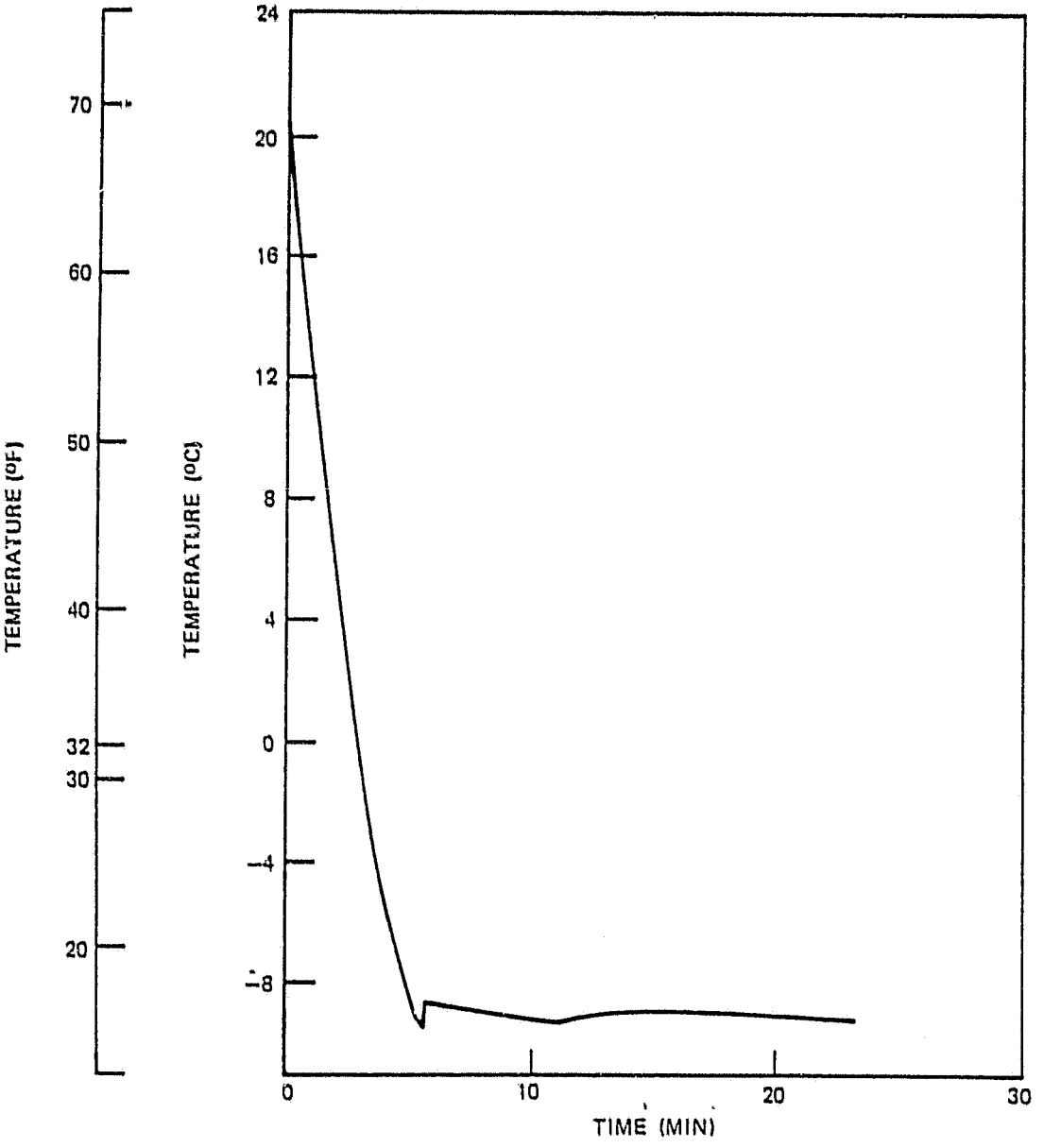

FIG. 16

78-05-55-4

TEMPERATURE VERSUS TIME FOR 16% KHF_2

MODERATE COOLING

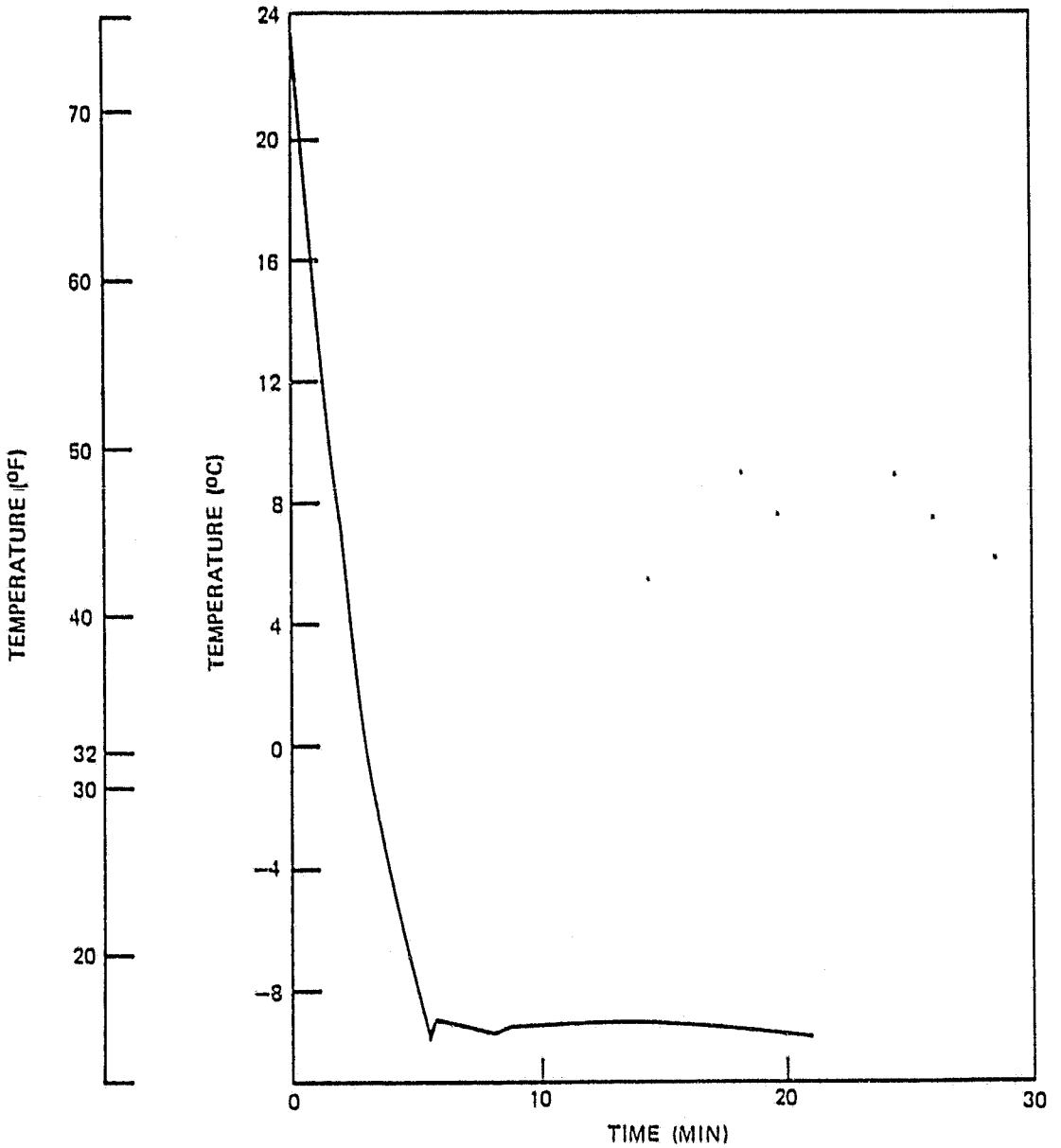

FIG. 17

78-05-55-5

TEMPERATURE VERSUS TIME FOR 18% KHF_2

MODERATE COOLING

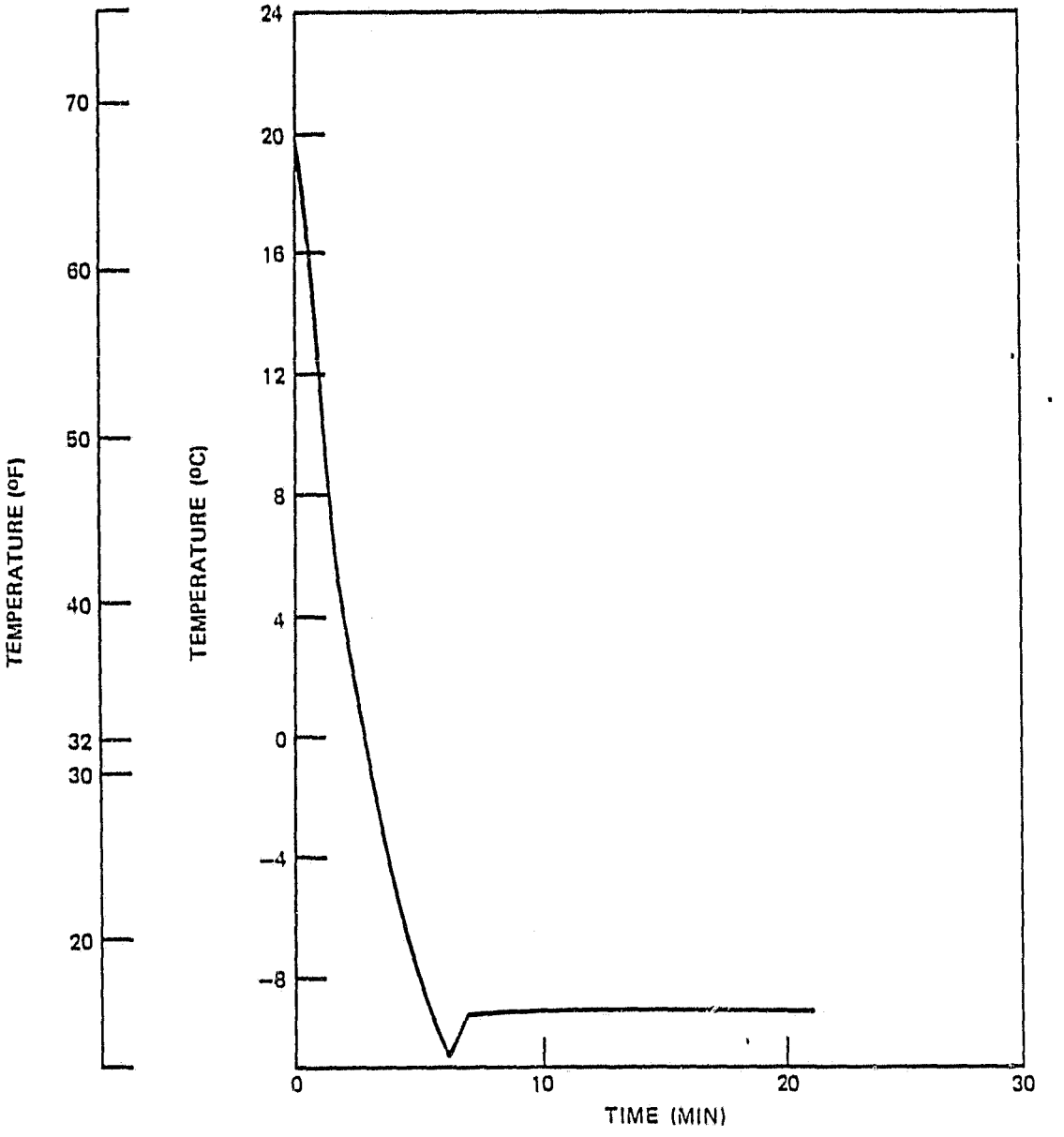

FIG. 18

78-05-55-6

TEMPERATURE VERSUS TIME FOR 19% KHF_2

MODERATE COOLING

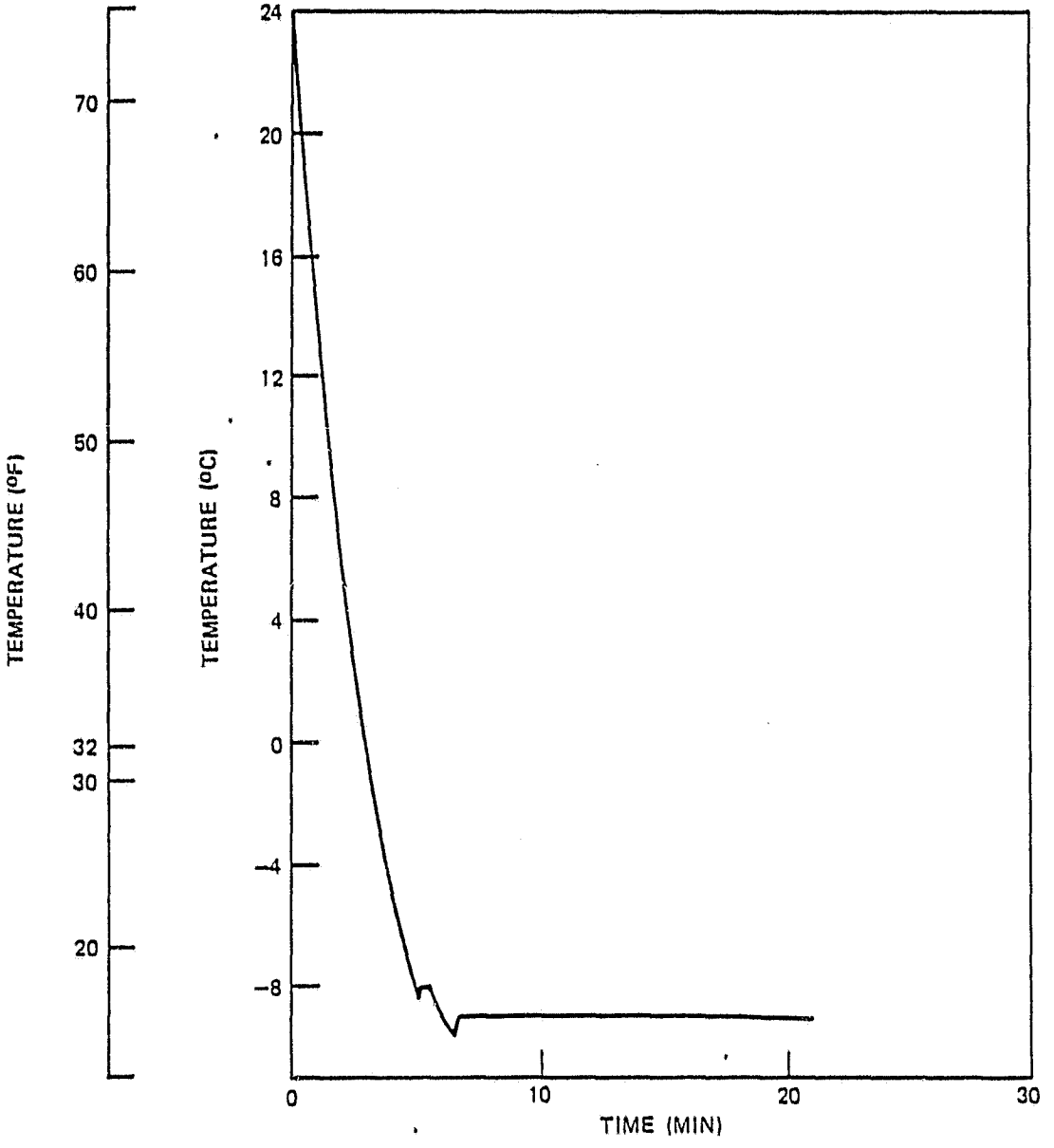

FIG. 19

78-05-55-7

TEMPERATURE VERSUS TIME FOR 25% KHF_2

MODERATE COOLING

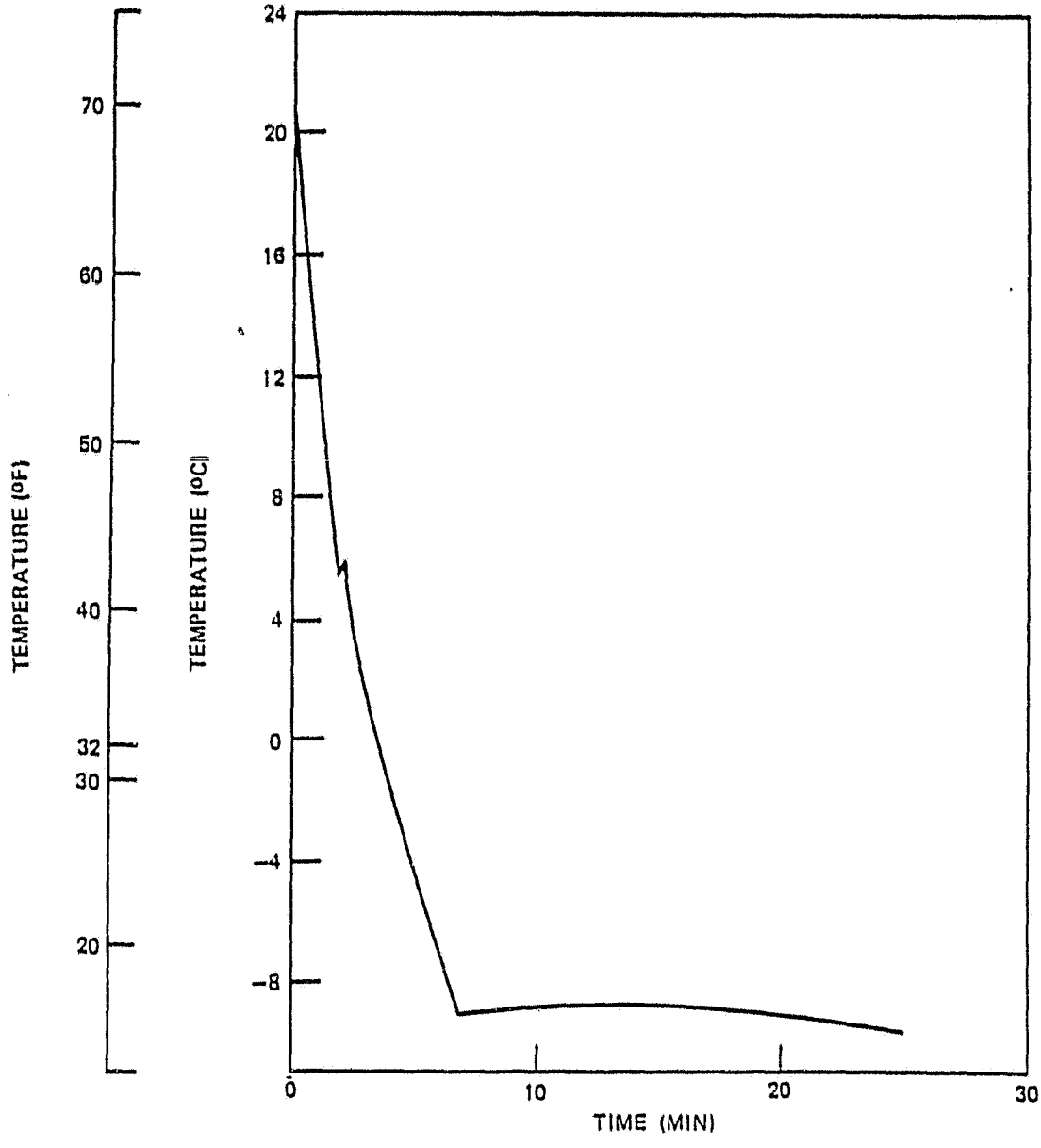

FIG. 20

78-05-55-8

TEMPERATURE VERSUS TIME FOR 5 PERCENT KHF_2

FAST COOLING

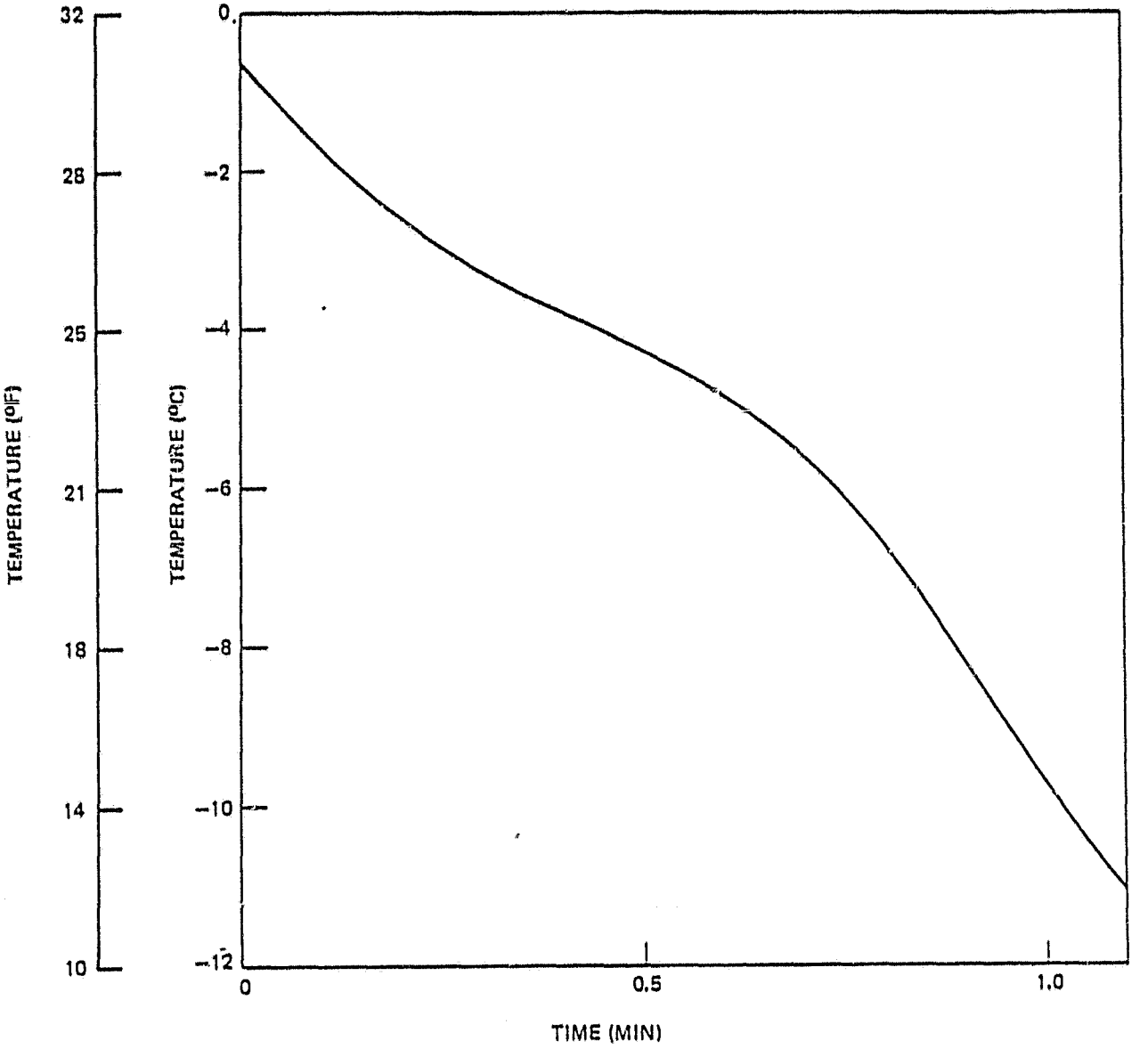

FIG. 21

78-06-68-1

TEMPERATURE VERSUS TIME FOR 10 PERCENT KHF_2

FAST COOLING

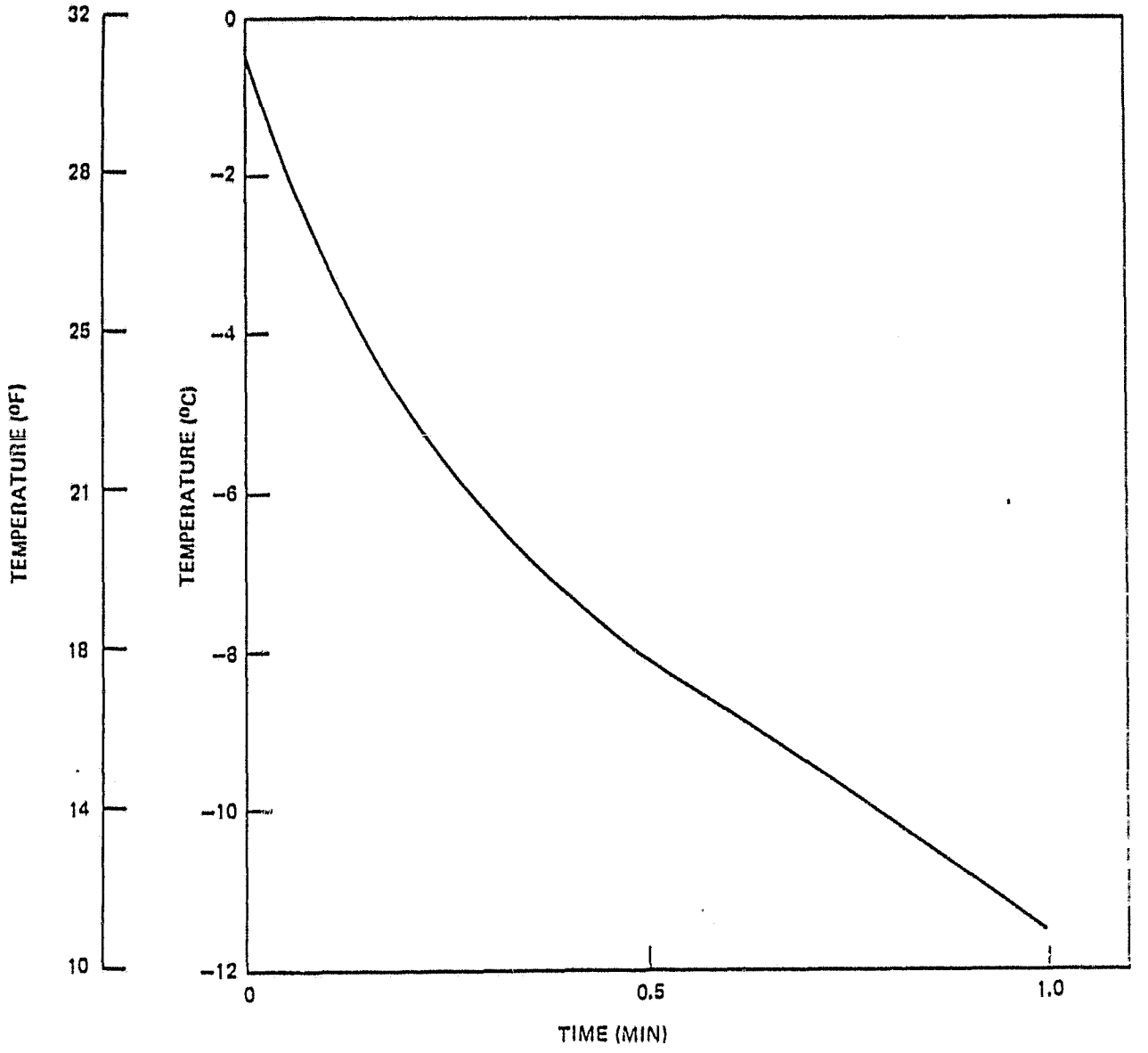

FIG. 22

78-06-68-2

TEMPERATURE VERSUS TIME FOR 15 PERCENT KHF_2

FAST COOLING

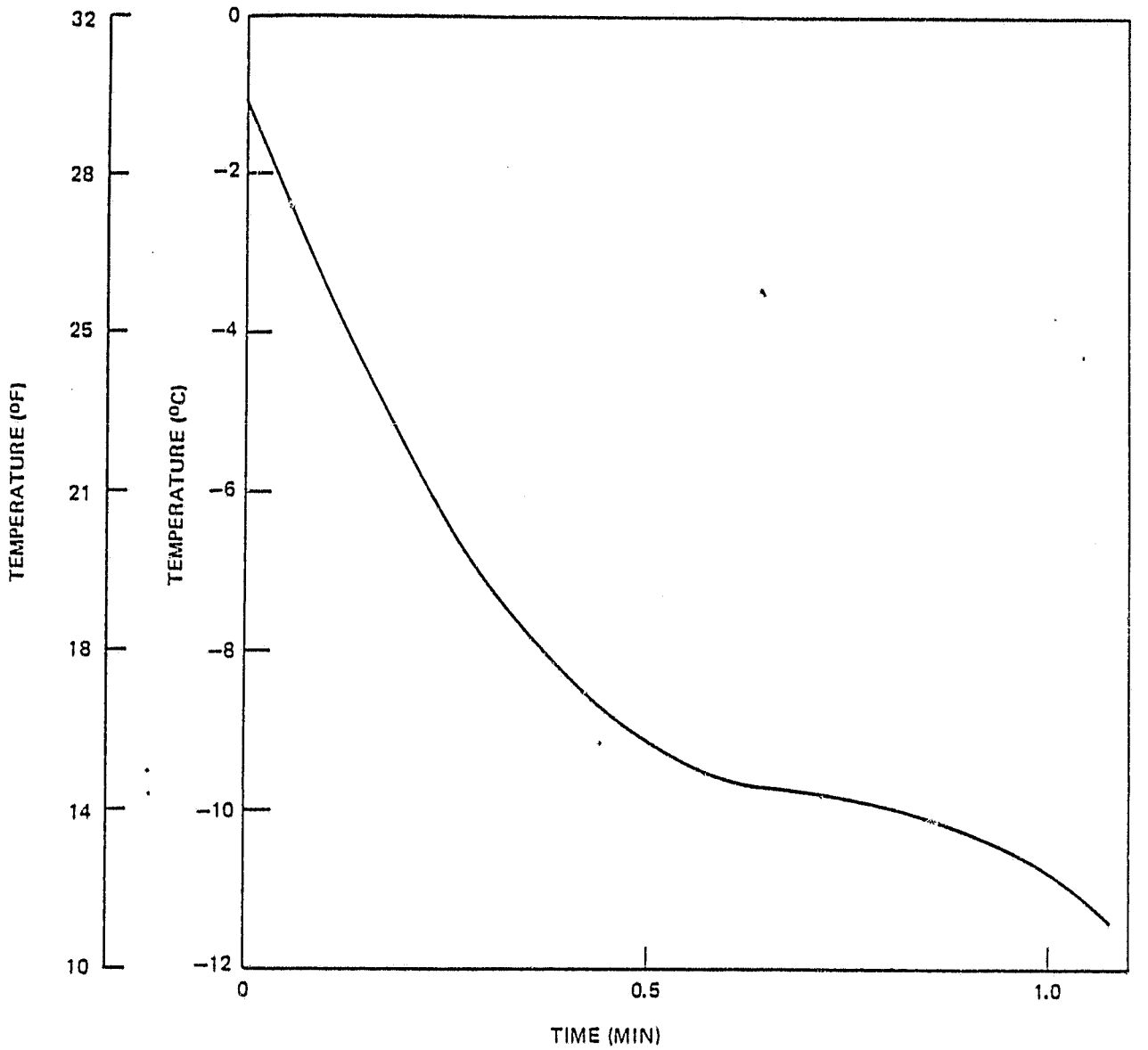

FIG. 23

78-06-68-3

TEMPERATURE VERSUS TIME FOR 16 PERCENT KHF_2

FAST COOLING

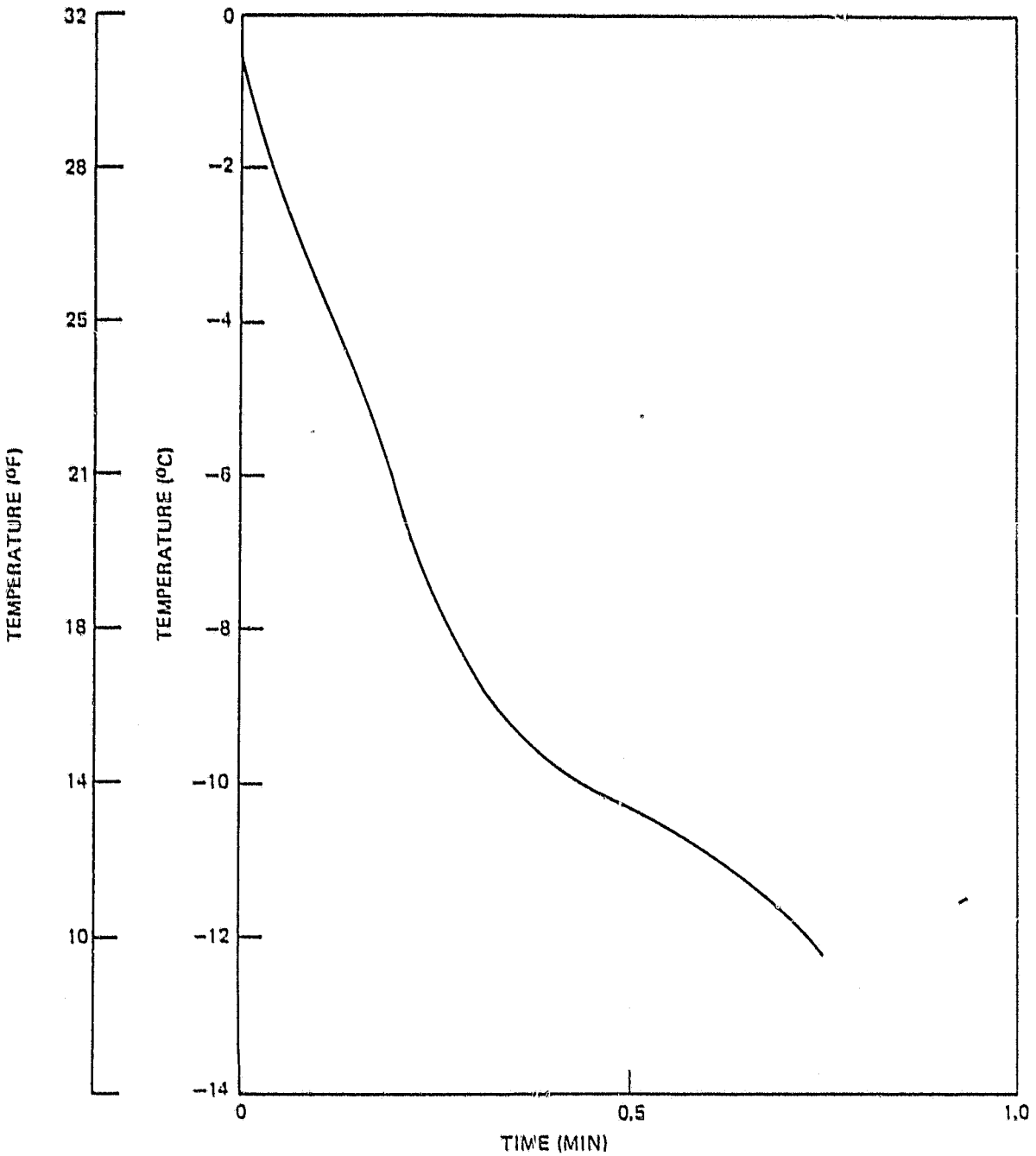

FIG. 24

79-06-68-1

TEMPERATURE VERSUS TIME FOR 18 PERCENT KHF_2

FAST COOLING

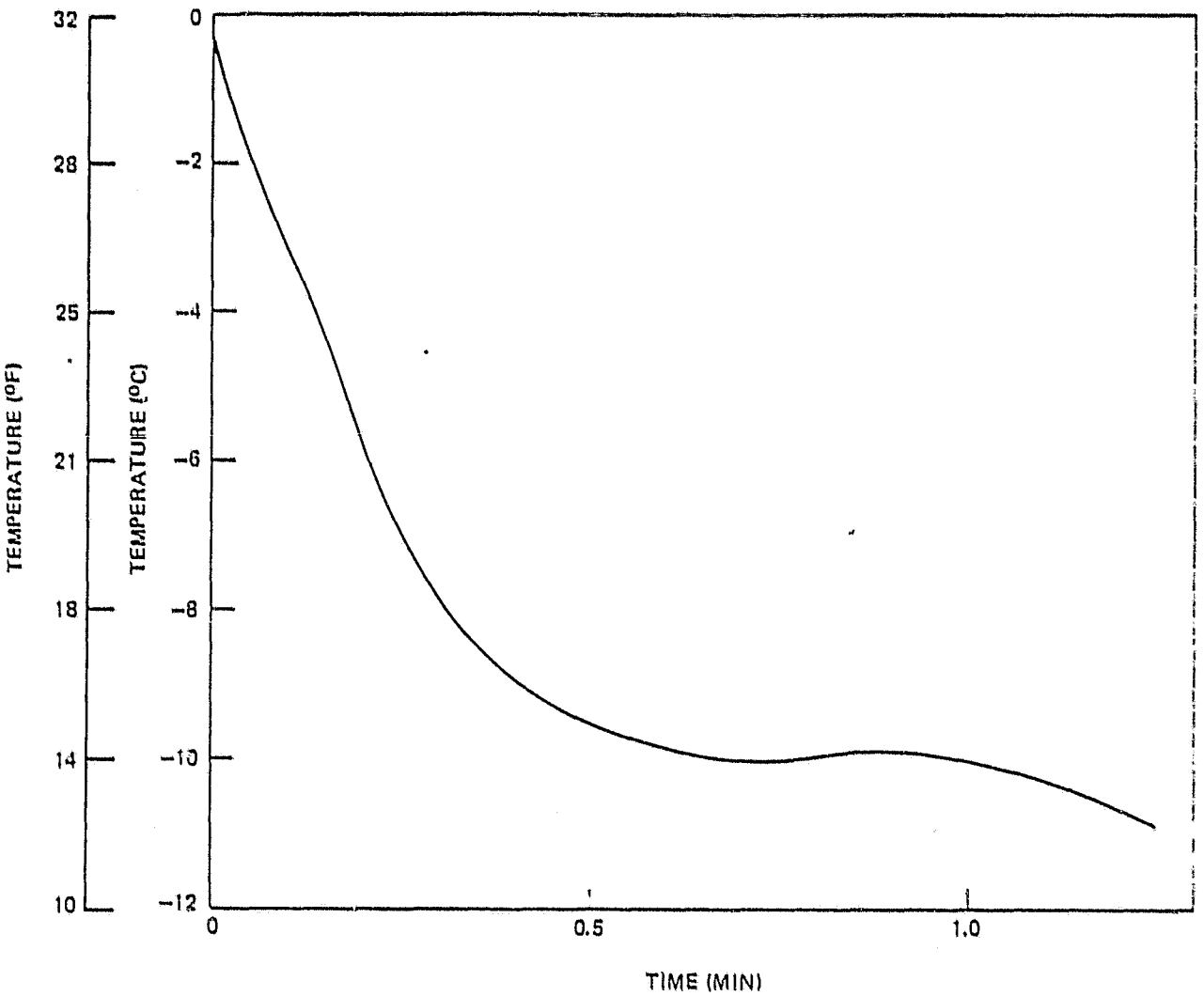

FIG. 25

78-06-68-5

TEMPERATURE VERSUS TIME FOR 19 PERCENT KHF_2

FAST COOLING

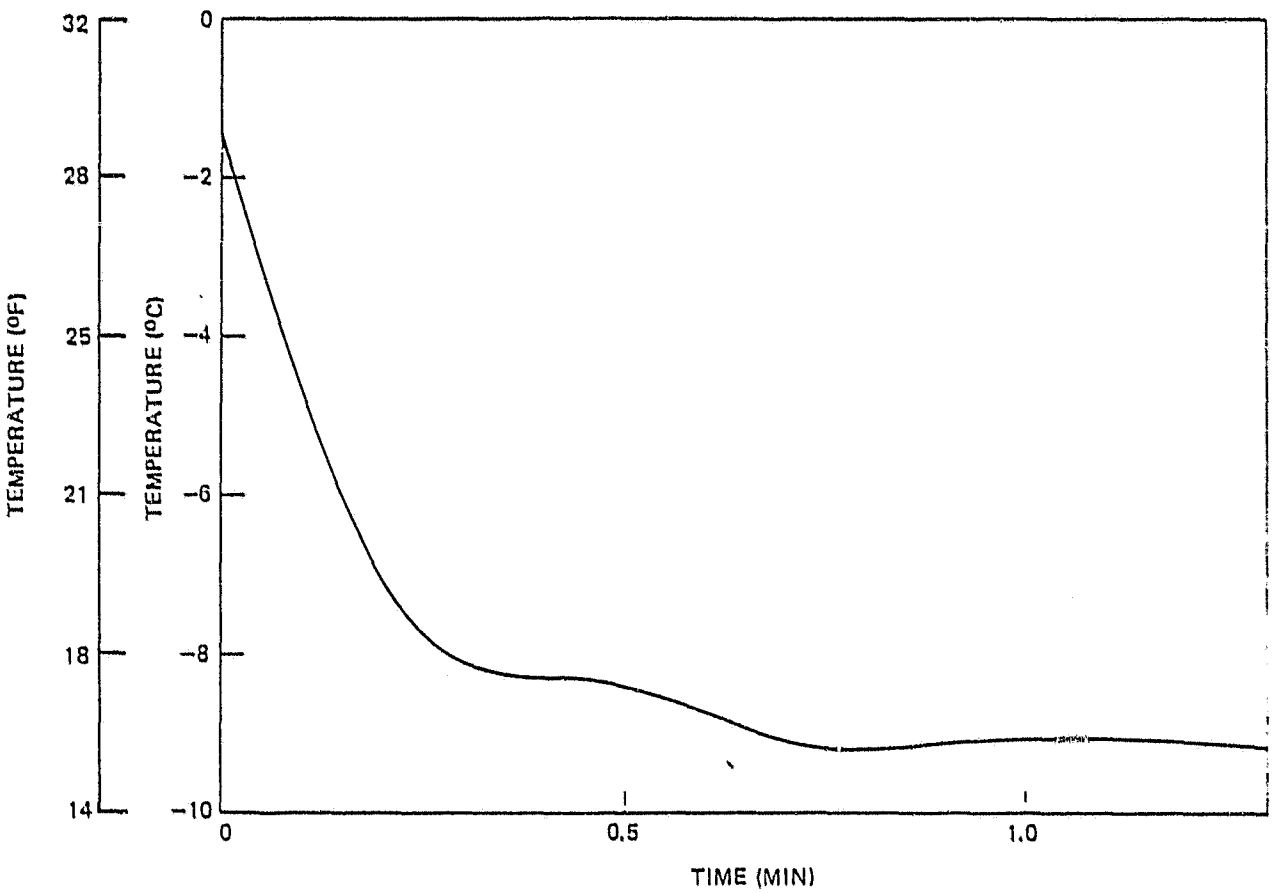

FIG. 26

TEMPERATURE VERSUS TIME FOR 20 PERCENT KHF_2

FAST COOLING

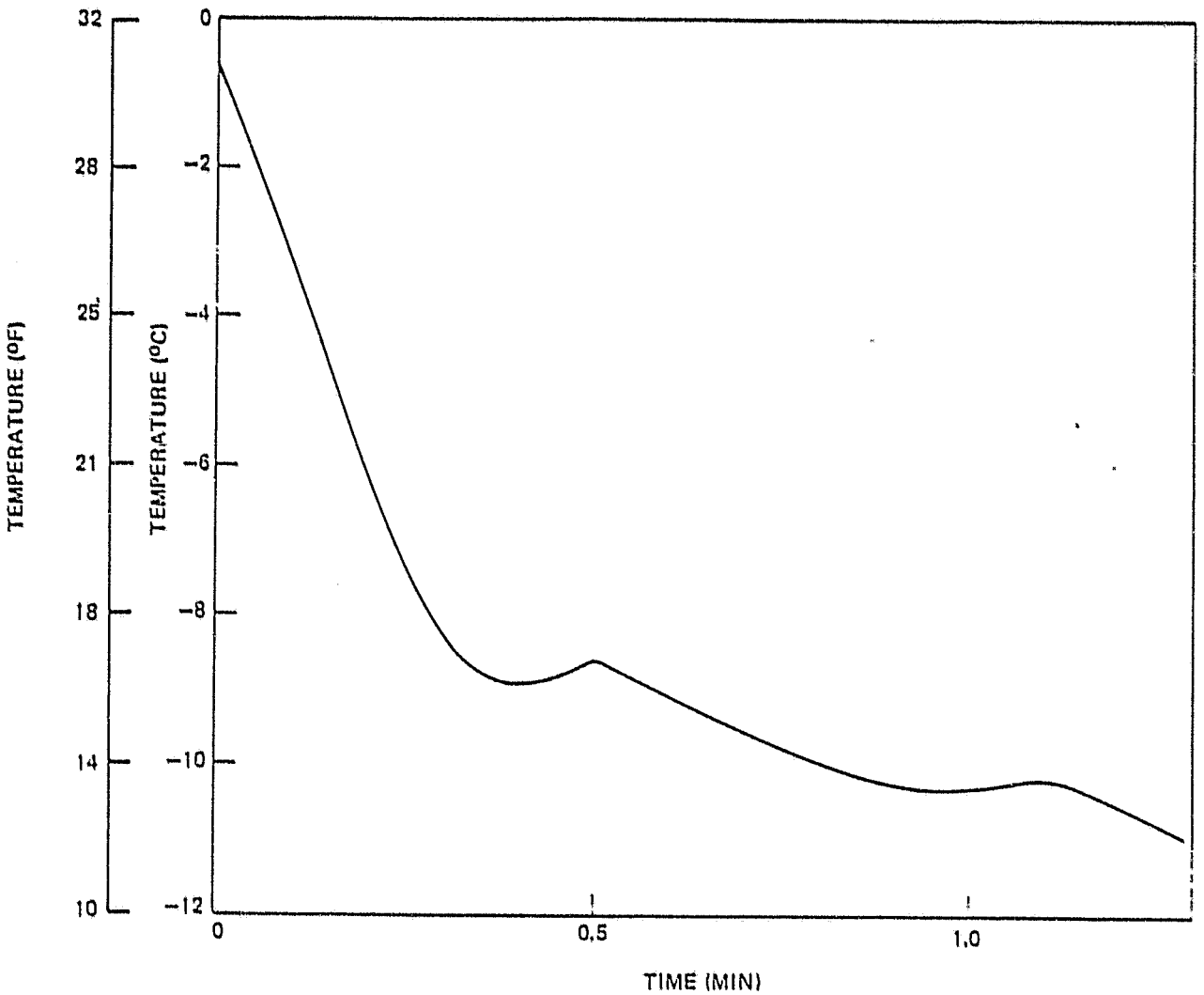

FIG. 27

78-06-68-7

TEMPERATURE VERSUS TIME FOR 25 PERCENT KHF_2

FAST COOLING

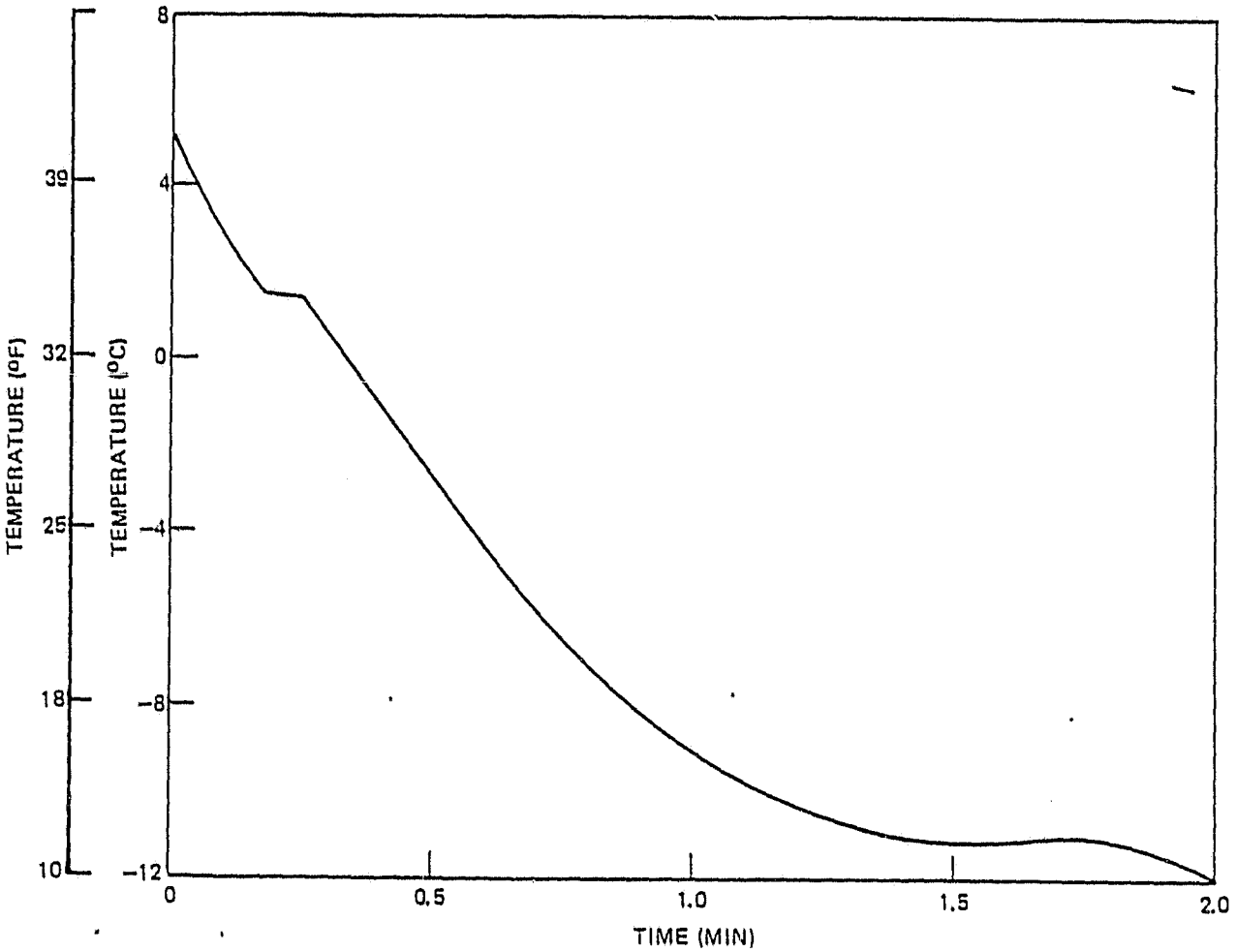

FIG. 28

TEMPERATURE VERSUS TIME FOR 30 PERCENT KHF_2

FAST COOLING

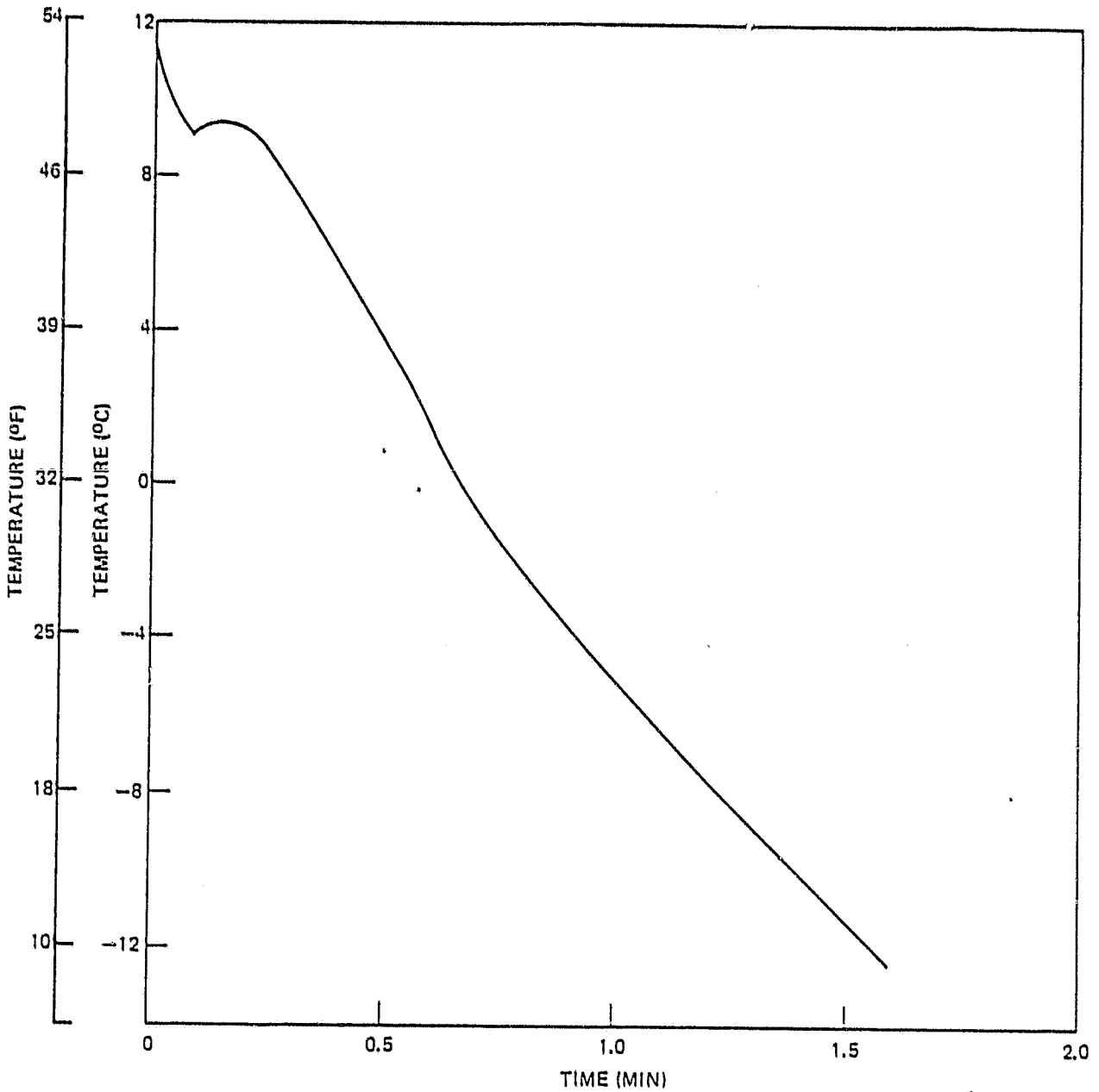

FIG. 29

78-06-68-9

TEMPERATURE VERSUS TIME FOR 40 PERCENT KHF_2

FAST COOLING

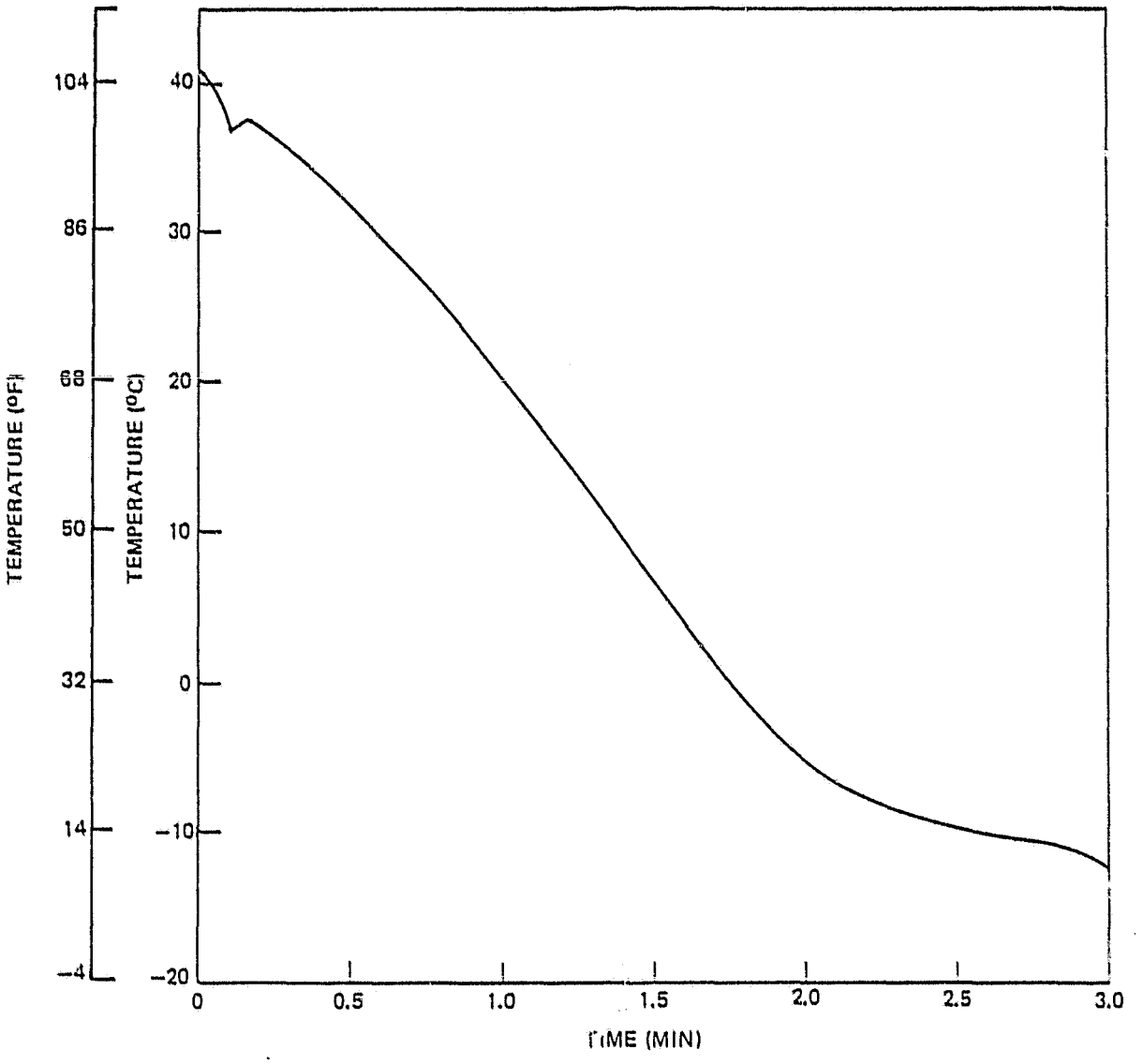

FIG. 30

78-06-68-10

The degree of supercooling is essentially zero for the fast cooling rate and small for the moderate cooling rate at composition less concentrated than the eutectic composition. However, the degree of supersaturation that occurs at higher salt concentrations at the first transition which represents the solubility limit for KHF_2 was greater for the fast cooling rates that for the slow rates. The fast cooling rates tended to overshoot the solubility limits and supersaturation was observed for this transition. By contrast, the super-saturation observed at the solubility limit transition at the fast cooling rates was not observed for slow cooling rates while the freezing point transitions at the lower concentrations exhibit just the opposite behavior as a function of cooling rate.

At the fast cooling rates the measured transition temperatures tended to be lower than the corresponding transition temperatures measured at slower rates. The measured transition temperatures are shown in Table 6. This tendency to overshoot the equilibrium transition temperatures is partly caused by the inability of the apparatus to respond to the rapidly changing temperatures.

TABLE 6

COMPARISON OF MEASURED TRANSITION TEMPERATURES AT SLOW, MODERATE AND FAST COOLING RATES

Concentration (wt %)	Slow Cooling Rate 0.3°C/min (0.5°F/min)				Moderate Cooling Rate 4°C/min (7°F/min)				Fast Cooling Rate 14°C/min (25°F/min)			
	Freezing Point		Eutectic Point		Freezing Point		Eutectic Point		Freezing Point		Eutectic Point	
	°C	(°F)	°C	(°F)	°C	(°F)	°C	(°F)	°C	(°F)	°C	(°F)
5	-2.6	(27.3)			-3.5	(25.7)			-5.6	(21.9)		
10	-5.6	(21.9)			-5.7	(21.7)			-7.8	(18.0)		
13	-7.3	(18.9)			-7.4	(18.7)			-8.1	(17.4)		
15	-8.9	(16.0)	-8.9	(16.0)	-8.5	(16.7)	-9.0	(15.8)			-9.4	(15.1)
16	-9.1	(15.6)	-9.1	(15.6)	-8.9	(16.0)	-9.1	(15.6)			-9.8	(14.4)
18	-8.3	(17.1)	-8.8	(16.2)			-9.1	(15.6)	-9.0	(15.8)	-9.9	(14.2)
19	-4.9	(23.2)	-8.8	(16.2)	-7.8	(18.0)	-8.9	(16.0)	-8.2	(17.2)	-9.1	(15.6)
20	-3.2	(26.2)	-8.0	(17.6)	-3.2	(26.2)	-8.7	(16.3)	-8.6	(16.5)	-10.2	(13.6)
25	9.0	(48.2)	-8.8	(16.2)			-8.9	(16.0)	1.4	(34.5)	-11.1	(12.0)
30	23.4	(74.1)	-8.6	(16.5)			-8.7	(16.3)	9.4	(48.9)		
40	44.3	(111.7)	-8.9	(16.0)	39.7	(103.5)	-9.1	(15.6)	37.5	(99.5)	-10.0	(14.0)

DISCUSSION

Equilibrium Phase Diagram

All compositions between 5 and 40% KHF_2 exhibited two transitions except for the 15% solution which exhibited only one. The second transition at all compositions as shown in Table 6 for the slow cooling case came between -8.0°C (17.6°F) and -9.1°C (15.6°F), a very narrow range. This transition represents the eutectic point and is the lowest temperature at which the KHF_2-H_2O system can exist as 100% liquid. The composition which corresponds to the eutectic composition is 15 wt% KHF_2. Although this solution does not form a compound, both the salt and the solvent precipitate out together, mixing intimately at the eutectic temperature of -8.7°C (16.3°F). At compositions less concentrated than the eutectic composition (hypoeutectic) the solid appearing first is water-ice and the liquidus is a freezing point curve. At compositions more concentrated than the eutectic composition (hypereutectic) the first solid to appear on cooling is KHF_2 salt, and the liquidus curve on that side is a solubility curve. No evidence of compound formation in particular, hydrate formation was found. No evidence of solid transitions or metastable states were found since all of these conditions would produce breaks in the solidus or liquidus curves in Figure 12.

The diagram for the KHF_2-H_2O system is typical of that of two components that are completely miscible in the liquid state and whose solid phases consist of pure components. In our case the completely miscible liquid phase is KHF_2 solution and the solid phases are water-ice for the hypoeutectic compositions and KHF_2 for the hypereutectic compositions. The significant finding for this system is the fact that a eutectic point exists and that its composition is 15 wt%, while the solution that in previous work (Reference 1) had been shown to have the highest heat absorption was 20 wt% (25g KHF_2 per 100g H_2O).

Non-Equilibrium Effects

Three different cooling rates were used with the first and slowest rate, about 0.3°C/min (0.50°F/min) used for construction of the equilibrium diagram. The faster rates, 4°C/min (7.2°F/min) (moderate) and 14°C/min (25.2°F/min) (fast) were used to assess the effect of fast freezing on the phase diagram in an attempt to reconcile the differences in heat absorption obtained with different measuring techniques The compositions of 19% and 20% exhibited some supercooling at the second transition as shown in Table 5, 2.2°C (4.0°F) for the

19% solution and 3.3°C (5.9°F) for the 20% solution. This supercooling was smaller at the moderate cooling rate, 0.5°C (0.9°F) for the first transition and 0.9°C (1.6°F) for the second for the 19% solutions. The 20% solution exhibited almost no supercooling or supersaturation at the fast cooling rate, which represents the rate of cooling used for the heat absorption measurement (Reference 1) at UTRC. It is doubtful that the small difference in the amount of supercooling or supersaturation for the 20% solution can have an effect on the magnitude of the heat absorption when the temperature is raised. However, the temperatures of the transitions obtained at the three cooling rates did differ markedly as shown in Table 6. At the slow cooling rate the 20% solution underwent transitions at -3.2°C (26.2°F) and at -8.0°C (17.6°F) while at the fast cooling rate these transitions occurred at -8.6°C (16.5°F) and -10.2°C (13.6°F). The first transition represents precipitating KHF_2 and the second transition KHF_2 and water-ice precipitates out together. Therefore at slow cooling rates, some salt comes out of solution before water-ice appears while at fast cooling rates, salt and water-ice precipitate together.

Practical Application of the KHF_2-H_2O Systems

The requirements of a heat absorption system normally include a reasonable limit on the elapsed time of absorption for a given heat input. The KHF_2 system involves melting which is a fairly rapid process, but it also requires the dissolution of a salt. The salt in this case is KHF_2 which has a large negative heat of solution and therefore its solubility is very dependent on temperature. The phase diagram in Figure 12 shows that the liquidus curve for hypereutectic solutions is very steep with 25g of KHF_2/100g H_2O (0.25 lb/lb H_2O) (20%) dissolving at 0°C (32°F) and 50g of KHF_2/100g H_2O (0.5 lb/lb H_2O) (33%) dissolving at 30°C (86°F). Another factor affecting the rate of dissolution of KHF_2 is the fact that the large negative heat of solution is caused by a small solute-solvent interaction as explained in Reference 3. The driving force for dissolution of KHF_2, as in all equilibria, is a minimum in the free energy of the system. In this case, the increase in entropy resulting from the dispersion of the solid KHF_2 lowers the free energy more than the increase in energy required for the dispersion. Thus, although the salt does dissolve, the absence of a hydrating mechanism and the reliance of the mechanism on entropy effects almost exclusively would indicate that a slow rate of dissolution is to be expected. Even when stirring is used, the increased movement of salt and the smaller salt particles does not increase the rate of dissolution, but merely produces a suspension of fine particles.

These two effects, the limited solubility at low temperatures and the slow dissolution rate combine to limit the maximum heat absorption obtained to long controlled experiments such as those in a sensitive calorimeter.

The findings of the rate of cooling experiments as far as supercooling and supersaturation are concerned do not indicate any reason why the rate of cooling should effect the heat absorption, however, the lower first transition

temperatures for the 20% solution on fast cooling means that the solid that precipitates will be an intimate mix of salt and water-ice. This mixture would probably dissolve at a faster rate upon heating than the mixture that precipitates on slow cooling.

Both of these findings have implications for the optimum solution composition to be chosen for heat absorption applications. First, it appears advantageous for an intimate mix of salt and water-ice to precipitate on cooling in order to facilitate the dissolution upon heat absorption. This can be assured through the use of the eutectic mixture (15% KHF_2) since as shown in Table 6, the eutectic transition is virtually independent of the cooling rate. Therefore, an intimate mix of salt and water-ice always appears on cooling the eutectic mixture, thus assuring the best possible dissolution rate. Second, the eutectic mixture remains liquid at the lowest temperature, and therefore, there is a greater opportunity for the salt to dissolve. The 15% KHF_2-H_2O mixture remains liquid down to about -9°C (15.8°F) while the 20% solution upon which earlier work is based remains liquid only to -3.2°C (26.2°F). The heat absorption capacity of the 15% solution can be estimated by interpolation between the values obtained for the more concentrated solutions and the value for pure water. This value is about 450 J/g (107 cal/g).

REFERENCES

1. Roebelen, Jr., G. J., and J. D. Kellner. Design, Development and Fabrication of a Prototype Ice Pack Heat Sink Subsystem - Potassium Biflouride/Water Solution Investigation, Final Report, CR151982, SVHSER 7163.

2. "Textbook of Physical Chemistry" - Glasstone, D. Van Nostrand Co., Inc. 1946.

3. Kellner, J. D.: "Improved Thermal Storage Material for Portable Life Support Systems," ASME Paper 75-ENAS-40, 1975.